

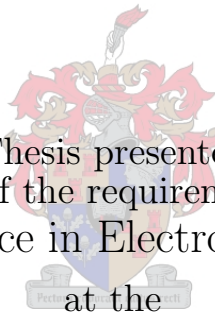


UNIVERSITEIT•STELLENBOSCH•UNIVERSITY
jou kennisvennoot • your knowledge partner

Implementation of a Low-cost FM-CW Radar

by

Jonathan G Hoole



Thesis presented
in partial fulfilment of the requirements for the degree of
Master of Science in Electronic Engineering
at the

University of Stellenbosch

Department of Electrical and Electronic Engineering,
University of Stellenbosch,
Private Bag X1, 7602 Matieland, South Africa.

Supervisor: Prof. KD Palmer

March 2008

Declaration

I, the undersigned, hereby declare that the work contained in this thesis is my own original work and that I have not previously in its entirety or in part submitted it at any university for a degree.

Signature:

JG Hoole

Date:

Abstract

Modern technology is reducing the cost of electronic devices. The speed of these devices and their reliability is improving. They can be used to implement low cost systems without compromising performance.

The design of two linear FM-CW radars using direct digital synthesis (DDS) is discussed. The use of the DDS simplifies the generation of the linear frequency sweep that is required. The systems are analysed mathematically and by computer simulation, before being implemented in hardware.

The first system is to be used to measure the position of pedestrians, at short range. The other system is to be used as a ground penetrating radar to measure the depth of objects located close to the surface.

The design of a micro-strip patch array with a corporate feed network is also discussed. The antenna is constructed, measured and used in the pedestrian measurement system.

Both systems are tested and used for initial radar measurements and the results obtained are presented.

Opsomming

Moderne tegnologie verminder die koste van elektroniese toestelle. Die spoed van hierdie toestelle, sowel as hul betroubaarheid verbeter voortdurend. Hulle kan gebruik word om lae-koste sisteme te implementeer sonder om werkverrigting te verswak.

Die ontwerp van twee liniere FM-CW (Frequency Modulated Continuous Wave) radars deur gebruik te maak van direkte digitale sintese (DDS) word bespreek. Die gebruik van die DDS vereenvoudig die benodigde opwekking van n liniere frekwensieswaai. Die stelsels is wiskundig geanaliseer, sowel as deur rekenaarsimulasie, voordat dit in hardeware geïmplementeer is.

Die eerste stelsel se doel is om die posisie van voetgangers te meet teen kort afstande. Die ander stelsel se doel is om as 'n grond-deurdringende radar om die afstand van voorwerpe na aan die oppervlak te meet.

Die ontwerp van 'n mikrostrook plak-antenna skikking met 'n korporatiewe voernetwerk is ook bespreek. Die antenna is vervaardig, gemeet en gebruik in die voetganger-afstandskat-sisteem.

Beide sisteme is getoets en gebruik vir aanvangsmetings vir radar en die resultate word aangebied.

Acknowledgment

A word of thanks to the following:

- The CSIR for the financial contribution without which this project would never have been possible.
- Professor K.D. Palmer, thanks for your enthusiasm, encouragement, and for sharing your knowledge.
- My parents for support, encouragement, and for always believing in me.
- The experts at *RRS* who helped me to understand the basics.
- Jacques at *ETSE* for the loan of the components that kick-started the practical aspect of my work.
- All the guys in the *Molshoop* especially Martin, it's good to know that I wasn't the only one who struggled.
- Jaco for all the distracting coffee breaks when I needed them the most.
- JP for proofreading my thesis.
- Andrew for helping with measurements and acting as a radar target.

Contents

Declaration	ii
Abstract	iii
Opsomming	iv
Acknowledgment	v
Contents	vi
List of Figures	ix
List of Tables	xi
Nomenclature	xii
1 Introduction	1
1.1 Project Description	2
1.2 Thesis Outline	2
2 System Design and Simulation	4
2.1 FM-CW Radar Theory and Block Diagram	4
2.1.1 Mathematical Parameter Calculation	8
2.2 Data Processing	12
2.2.1 Sampling and FFT	12
2.2.2 Windowing	13
2.2.3 Sensitivity Frequency Control	15
2.3 Simulations	18
2.3.1 Simulation Results	21
2.3.2 Simulation Results With Noise	25
2.4 Experimental Proof of Concept	26
2.4.1 Setup	26
2.4.2 Results	28
2.5 Conclusion	29

3	Sub-System Components	31
3.1	Direct Digital Synthesizer	31
3.2	Phase Locked Loop	32
3.3	Local Oscillator	34
3.3.1	Phase noise	34
3.4	Analog	37
3.4.1	Voltage regulators	37
3.4.2	Amplifier	37
3.4.3	Mixer	38
3.4.4	Splitter	39
3.4.5	Filters	41
3.5	ADC	42
3.6	Conclusion	42
4	Antenna design	43
4.1	Patch	44
4.1.1	Array	47
4.2	Feed network	48
4.3	Measurements	51
4.4	Test Target	53
4.5	Other Antennas	54
5	Final Measurements	57
5.1	Pedestrians	57
5.1.1	Setup	57
5.1.2	Results	61
5.1.3	RCS Measurements	62
5.2	Ground Penetrating Radar	64
5.2.1	Setup	64
5.2.2	Results	67
5.3	Local Oscillator	69
5.4	Conclusion	70
6	Conclusion	72
6.1	Conclusion	72
6.2	Further Development	74
	Bibliography	76
A	Simulation Functions	78
A.1	Radar Simulation	79
A.2	DDS	81
A.3	Approximate DDS	84

CONTENTS

viii

A.4 Radar Equation	86
A.5 AGC	87
A.6 Filter	88
A.7 Window and sampling	89

List of Figures

2.1	Block Diagram of simulated radar	5
2.2	Signal with increasing frequency	7
2.3	Triangular FM	7
2.4	Sawtooth FM	9
2.5	Windowing functions	14
2.6	Windowing functions	14
2.7	Effect of windowing functions on simulated radar	15
2.8	SFC Schematic	16
2.9	Frequency response of SFC filter	17
2.10	Block diagram for simulations	19
2.11	Simulations with different windowing functions	22
2.12	Simulation results without noise	23
2.13	The effect of Sensitivity Frequency Control	24
2.14	Plot of simulation results comparing the true linear frequency sweep v the DDS output signal	24
2.15	Simulation results with noise	26
2.16	Block diagram as used for the experimental proof of concept	27
2.17	Photo of proof of concept experiment	27
2.18	Photo of proof of concept Target	28
2.19	Measurement Results	29
3.1	Block diagram of DDS	32
3.2	Block diagram of DDS with frequency accumulator	32
3.3	Block diagram of PLL	33
3.4	LO and DDS Spectra	36
3.5	Measured S-parameters of Mini-Circuits amplifier	38
3.6	Splitter Measurements - Magnitude	40
3.7	Splitter Measurements - Phase	40
3.8	Filter Measurements	42
4.1	Antenna geometry showing feed network.	44
4.2	Definition of patch dimensions	45
4.3	Layers used for the Patch	45

4.4	Antenna Spacing in the Array	47
4.5	Feed Layout	49
4.6	S_{11} of feed network terminated with 100 Ω loads	50
4.7	Measured and simulated S11 of patch array	52
4.8	Measured and simulated Gain of patch array	52
4.9	Measured Radiation Pattern of Patch Array	53
4.10	Photo of Tri-hedral corner reflectors	54
4.11	Photo of Horn Antennas	55
4.12	Photos of GPR antenna	56
5.1	Block Diagram of radar	58
5.2	Photo showing the area in front of the radar	59
5.3	Diagram of the roof where the measurements were taken	59
5.4	Photo of the radar set-up showing the HF lab in the back ground	60
5.5	Measure Results with $\theta = 60^\circ$	61
5.6	Measure Results with $\theta = 70^\circ$	62
5.7	RCS measurement results	63
5.8	Block Diagram of simulated radar	64
5.9	Photo of GPR measurement set-up.	65
5.10	Position of antennas relative to storm water pipe.	65
5.11	Position of antennas relative to manhole cover.	66
5.12	Photo of GPR system and the manhole cover in position 27.	66
5.13	Measured results of GPR	67
5.14	Target at 7 kHz corresponds to target at 1 m below the surface	68
5.15	Target at 123 m in air or 41 m in ground	69
5.16	Measured spectrum of 1 GHz LO	70
6.1	Pedestrian Radar System	75

List of Tables

2-I	Filter Component Values	17
2-II	Window Function Taper Selection	21
2-III	Parameters for FM-CW Radar	30
3-I	Measured Amplifier Specifications	37
3-II	Mixer characteristics	39
4-I	Final dimensions of Patch Antenna	48
4-II	Line width on 1.52mm Rogers RO4003	50
5-I	Expected and measured Rx power of the RCS Measurements in dBm	63
6-I	GPR Component Costs	72
6-II	Pedestrian Radar Component Costs	73

Nomenclature

Abbreviations

ADC	= Analogue to Digital Converter
AGC	= Automatic Gain Control
AM	= Amplitude Modulation
B-H	= Blackman-Harris
CW	= Continuous Wave
DAC	= Digital to Analog Converter
DDS	= Direct Digital Synthesis
eirp	= Effective isotropic radiated power
EMI	= Electro-Magnetic Interference
EMC	= Electro-Magnetic Compatibility
FFT	= Fast Fourier Transform
FIR	= Finite Impulse Response
FM	= Frequency Modulation
FPGA	= Field Programmable Gate Array
GPR	= Ground Penetrating Radar
IF	= Intermediate Frequency
LNA	= Low Noise Amplifier
LO	= Local Oscillator
LUT	= Lookup Table
MTI	= Moving Target Indicator
PLL	= Phase-Locked Loop
PWM	= Pulse Width Modulation
QT	= Quarter wavelength Transformer
RCS	= Radar Cross Section

RF	= Radio Frequency
Rx	= Receive
SFC	= Sensitivity Frequency Control
STC	= Sensitivity Time Control
Tx	= Transmit
VCO	= Voltage Controlled Oscillator
WIMAX	= IEEE 802.16 Wireless Standard

Chapter 1

Introduction

The first radar system, though not called radar, was patented more than 100 years ago, in 1904 [1]. Modern technology has however made radars considerably cheaper and more accurate.

In the introduction of the new edition of his book *Introduction to Radar Systems*, M.I. Skolnik states:

‘Chapter 3 of the second edition, on CW and frequency modulated CW radar, has been omitted because of the decreasing utilization of this type of radar. Low-power CW and frequency modulated CW radars will still be used for some special applications, and are briefly included...’ [1]

This gives the impression that frequency modulated continuous wave (FM-CW) radar is starting to loose ground to other types of radar. This is not the opinion of D.J. Daniells in *Ground Penetrating Radar* (GPR), he states:

‘The majority of GPR systems use an impulse time domain wave form and receive the reflected signal in a sampling receiver. However, more use has been made of FM-CW and stepped frequency radar modulation schemes in recent years and, as the cost of components decreases, it may be expected that more of these systems will be used, as their dynamic range can be designed to be greater than the time domain radar’ [2]

This clearly points to FM-CW becoming more popular, especially in GPR applications.

The conflicting opinions in literature from Skolnik and Daniels [1; 2] about the future of FM-CW give rise to questions that need to be investigated. The quote from Daniels is newer and he might be convinced that the DDS is a factor that is causing FM-CW to be making an impact again, especially on the low-cost radar front [3]. In the previous version of his book, Skolnik says that FM-CW is not particularly well suited for applications where many targets need to be resolved or in areas where there is a high amount of clutter.

1.1 Project Description

The aim of this project was to determine whether new direct digital synthesis (DDS) technology can be used as the base for low cost, high performance linear FM-CW radar systems.

The system should be analysed mathematically, and simulated. Suitable components should be researched and the antennas will need to be designed. The system should be designed and built to be used as a radar demonstration in undergraduate courses.

The system specifications are: range resolution of 1 m, with a maximum range 1000 m, with pedestrians as the target. It is to be operated from a laptop computer. An analog to digital converter (ADC) will therefore be required to capture the data. An FFT is then to be used to calculate the range to the target [4].

A second system should also be built to determine the suitability of the system to GPR [5]. This system will use as many common components from the first system as possible.

1.2 Thesis Outline

A brief explanation of the theoretical and mathematical, working of a FM-CW radar is presented in **Chapter 2**. A general block diagram is presented which is expanded for use in the two systems, pedestrian radar and GPR. The design is verified by simulation. A few measurements of a practical system is also given as a proof of concept.

Chapter 3 gives a detailed description of the sub-system components.

Each of the blocks of the block diagram are discussed separately with suitable components being chosen to implement each block. The performance of each component and its influence on system performance is discussed.

The design and measurements of the antennas needed for the pedestrian radar are discussed in **Chapter 4**. The detailed design of a patch array with a corporate feed network is presented. The design of test targets are also briefly explained. Other antennas that were used for the project are also included. The antennas used for the GPR are pre-existing antennas.

The two systems were built and used for measurements. The measurements are presented in **Chapter 5**. The system performance is discussed and various factors that influences it are investigated.

The conclusion and recommendations for future work is presented in **Chapter 6**.

Chapter 2

System Design and Simulation

The aim of this chapter is to examine the theoretical details of FM-CW Radar, as well as to determine how the different variables affect the radar's performance. This is then used to simulate the radar. An experimental radar is also discussed in order to show that the system can be implemented with a practical system.

2.1 FM-CW Radar Theory and Block Diagram

A basic block diagram is shown in figure 2.1. FM-CW works on the mathematical principle that if you take two sinusoidal signals with different frequencies and multiply them, the result can be written as the sum of two sinusoidal signals. One having the sum, the other having the difference frequency of the original signals. Starting with the trigonometric identity given in equation 2.1, equations 2.2 and 2.3 can be derived for sinusoidal signals.

$$\cos(A) * \cos(B) = \frac{1}{2}\cos(A + B) + \frac{1}{2}\cos(A - B) \quad (2.1)$$

$$\cos(\omega_T t) * \cos(\omega_R t) = \frac{1}{2}\cos(\omega_T t + \omega_R t) + \frac{1}{2}\cos(\omega_T t - \omega_R t) \quad (2.2)$$

$$\cos(\omega_T t) * \cos(\omega_R t) = \frac{1}{2}\cos(\omega_s t) + \frac{1}{2}\cos(\omega_d t) \quad (2.3)$$

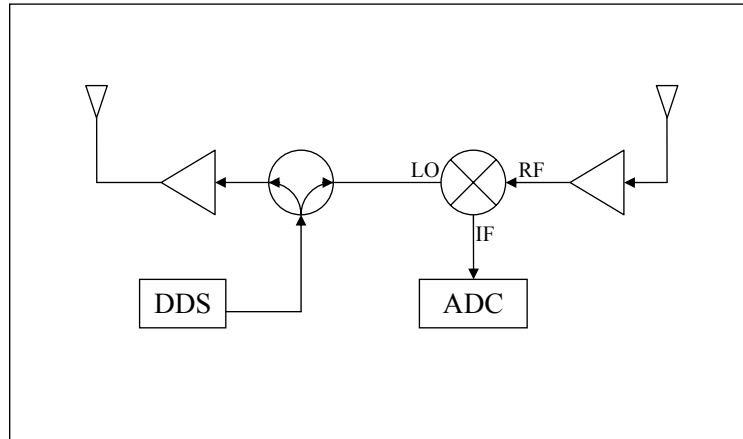


Figure 2.1: Block Diagram of simulated radar

Here $\omega_d = \omega_T - \omega_R$ is the difference frequency and $\omega_s = \omega_T + \omega_R$ the sum frequency.

In Equation 2.3 the information that is of interest is the difference frequency, which will generally be in the order of single MHz or less. The centre frequency will normally be more than 100 MHz. It is therefore not difficult to separate these frequencies by means of filtering.

Doppler radar is the simplest form of radar that is based on this principle. Doppler radar transmits a signal with a constant frequency. If this signal is reflected off a moving target, the frequency of the reflected signal will be different to that of the transmitted signal. The difference between the frequencies of the transmitted and received signals is given in equation 2.4, where F_D is the doppler frequency. This is equal to the difference frequency F_d that results from multiplying the transmit and received signals. By measuring F_d the speed of the target can be calculated.

$$F_D = \frac{2v_r}{\lambda} \quad (2.4)$$

Doppler radar does not give any information about the range to the target. To include range information, the transmit signal needs to be modulated. The modulation can be amplitude modulation (AM), frequency modulation (FM) or a combination of the two. Pulsed radar systems are an example

of amplitude modulated radar. For this project the focus is on frequency modulated radar. The amplitude of the transmitted signal is kept constant, so the system transmits continuously. The system is therefore referred to as a frequency modulated, continuous wave (FM-CW) radar.

When equation 2.3 and 2.4 are considered the centre frequency does not affect the range calculations. It does affect the doppler frequency. The choice of centre frequency is, however, not trivial. The higher the frequency, the easier it is to filter the sum frequency out of the signal, and the better the resolution will be for a specified % band width. Higher frequencies are also more difficult to work at and phase noise and oscillator drift are of greater concern. A frequency of 5.8 GHz is chosen for a centre frequency, as there is a licence free band (up to 2W eirp)[6] and it is one of the standard frequencies of WIMAX. This means that there are many available components at relatively low cost. The antennas are also smaller, and have higher gain, than low frequency antennas.

If the transmit frequency is increased with time at a known rate, the difference frequency is proportional to the time delay. Range can then be calculated, as shown in figure 2.2. For practical implementation the frequency cannot be increased indefinitely. Periodicity is therefore added. Normally triangular or saw tooth modulation is used, but it could be any periodicity. The periodicity can cause unwanted transient effects at any discontinuities that might exist. The transient effects are eliminated by not sampling while they are present. By doing this the Radar is not perfectly CW, but by limiting the frequency of the periodicity and having a short transients response, the the data that is lost can be less than 1 or 2 %.

For this project we will only be considering triangular and saw tooth modulation as other forms of modulation need more complex data processing to calculate the range. If the frequency is modulated sinusoidally, the difference frequency will also be sinusoidal. The FFT of a signal that has a sinusoidally modulated frequency will give a Bessel function. The range data is therefore calculated from the Bessel functions.

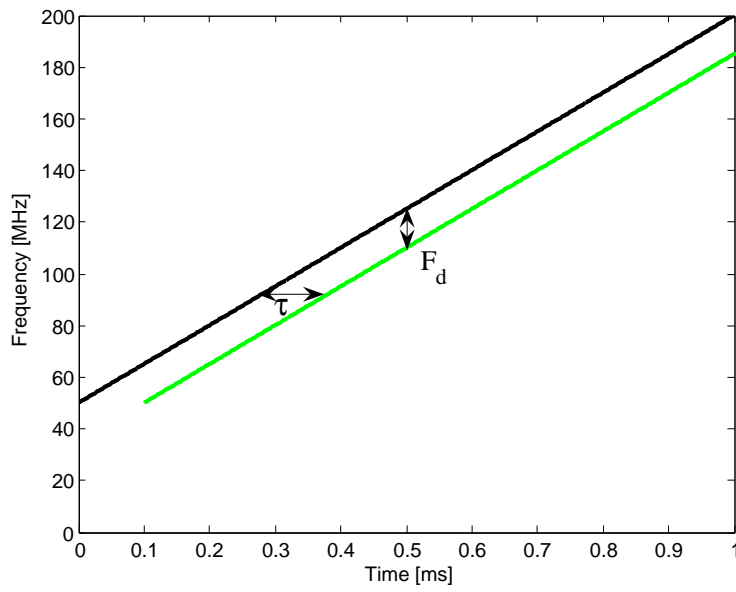


Figure 2.2: Signal with increasing frequency

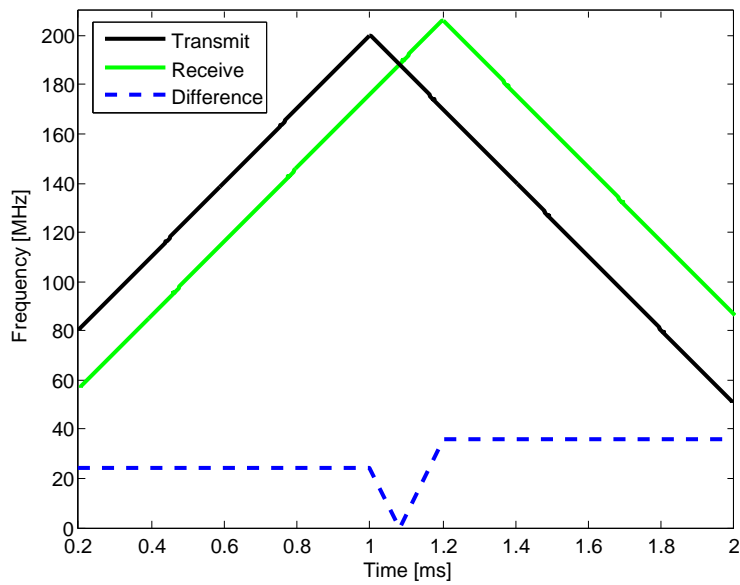


Figure 2.3: Triangular FM

In the theoretical frequency sweep there is an ambiguity between the change in frequency due to the range and the doppler shift. This is also true for the sawtooth modulated FM-CW, but if two sweeps of the triangular modulation is considered, this ambiguity can be resolved [7]. In Figure 2.3 the received signal is delayed and a doppler frequency is added. The doppler frequency can be calculated from the difference between F_d on the up and down slopes.

For the practical system designed the doppler assumed to be zero. The target would need to be travelling at 26 m/s for the doppler shift to be 1 kHz, which is equal to the frequency resolution of the FFT, see section 2.1.1. As the radar is to be used for the monitoring of pedestrians, it is unlikely for them to be moving that fast. Because doppler can be ignored, sawtooth modulation will be used. When using a DDS a sawtooth is the easiest to generate.

At the beginning of the sweep there will be a difference frequency, approximately equal to the bandwidth, between the transmit and receive signals, shown in figure 2.4. This is due to the step in frequency, and is one of the transient effects that need to be eliminated from the system. This difference frequency will be filtered out by the sensitivity frequency control (SFC) filter, see section 2.2.3 on page 15, and by the anti-aliasing filter of the ADC. If triangular modulation is used instead, this frequency is very low, as shown in figure 2.3.

The block diagram of a system that implements a basic FM-CW radar is given in figure 2.1. In the final system another block, a phase locked loop (PLL), is added to increase the centre frequency, see figure 2.16 on page 27.

2.1.1 Mathematical Parameter Calculation

There are many variables in the system, affecting the maximum range and resolution. These need to be calculated to satisfy the system specifications. The variables are all defined, below. Some are also shown in figure 2.4, followed by a mathematical explanation of the relationship between them.

- T_{sweep} is the total time over which the frequency is swept.
- T_{sample} is the time over which the ADC samples. The delay between the beginning of T_{sweep} and T_{sample} allows for transients and τ_{max} to pass.

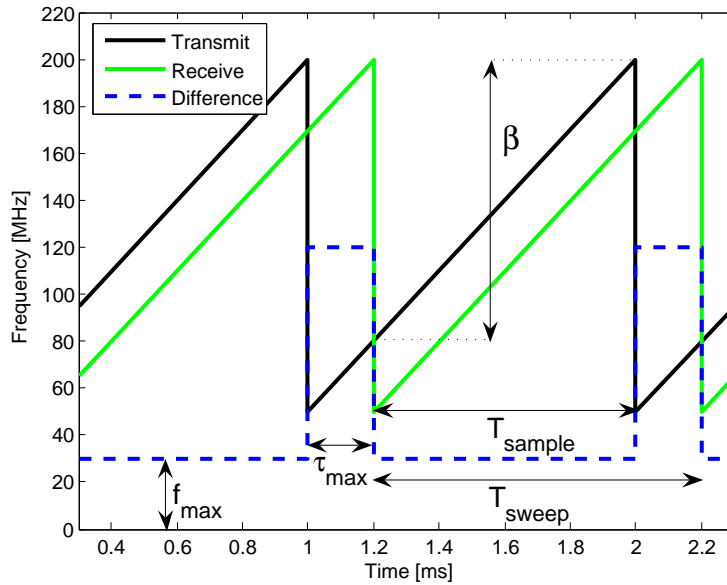


Figure 2.4: Sawtooth FM

- β is the frequency difference between the beginning and end of T_{sample} .
- S_r is the rate at which the frequency is swept ($\frac{\beta}{T_{sample}}$).
- R is the range [m] to the target.
- f is the frequency corresponding to a target at range R .
- R_{min} ; R_{max} are the minimum and maximum Range at which targets need to be identified, as per specification.
- f_{min} ; f_{max} are the difference frequencies corresponding to R_{min} and R_{max} , respectively.
- τ is the time delay due to propagation to a target at range R and back.
- τ_{max} is the time delay due to propagation to a target at range R_{max} and back.
- f_{sample} is the frequency of the ADC, so that f_{max} can be unambiguously sampled. $f_{sample} \geq 2 * f_{max}$.

- $N_{samples}$ is the number of samples that are available for the fast Fourier transform (FFT).
- ΔR is the Range resolution, the minimum distance at which 2 targets can be distinguished.
- Δf is the frequency spacing of the discrete frequency points after the FFT.

R_{min} , R_{max} and ΔR are given in the specifications of the project as 1 m, 1000 m, and 1 m, respectively. From these β and S_r are calculated, assigning values to f_{min} , f_{max} and f_{sample} .

For the mathematical explanations that follow T_{sample} is used, as all the calculations are based on the sampled data.

$$T_{sweep} \geq T_{sample} + \tau_{max} \quad (2.5)$$

$$S_r = \frac{\beta}{T_{sample}} \quad (2.6)$$

$$\tau = \frac{2R}{c} \quad (2.7)$$

The number of samples used for the FFT is equal to the number of frequency points that are calculated by the FFT.

$$N_{samples} = f_{sample} T_{sample} \quad (2.8)$$

The maximum frequency calculated by the FFT is equal to the sampling frequency. This means that the frequency resolution is given by

$$\Delta f = \frac{f_{sample}}{N_{sample}} = \frac{1}{T_{sample}} \quad (2.9)$$

The frequency corresponding to a target at range R is

$$f = S_r \tau = \frac{\beta}{T_{sample}} \frac{2R}{c} \quad (2.10)$$

The range R to a target can therefore be calculated from the frequency by

$$R = \frac{fT_{sample}c}{2\beta} \quad (2.11)$$

This results in the range resolution given by

$$\Delta R = \frac{\Delta f T_{sample} c}{2\beta} = \frac{T_{sample}}{T_{sample}} \frac{c}{2\beta} = \frac{c}{2\beta} \quad (2.12)$$

For a range resolution of 1 m a bandwidth of 150 MHz is therefore needed. For the GPR the resolution should be as high as possible and a bandwidth of 300 MHz is therefore used.

Having calculated the bandwidth, T_{sweep} now needs to be calculated. Given the maximum specified range of 1000 m, τ_{max} is calculated as 6.7 μs . Extra bandwidth that is swept before starting to sample is not used and because the data during this period is not sampled there is also unused power. This wasted power and extra bandwidth must be minimised. Typically τ_{max} should be less than 10% of T_{sweep} , and it is not uncommon for τ_{max} to be less than 1% of T_{sweep} [8]. By using a longer T_{sweep} , T_{sweep} and T_{sample} can be very close to equal, and a slower ADC can be used, as the difference frequency is lower.

The large dynamic range of the system suggests that the use of a slower ADC with a higher number of bits would be an advantage, as the higher number of bits per sample gives a greater dynamic range.

Target information can only be calculated once per T_{sweep} , as a complete set of $N_{samples}$ samples is needed. If the rate at which the target information is to be kept high T_{sweep} should be kept short, this will mean using a higher f_{max} .

An AD7760 ADC from Analog devices is chosen as it has 100 dB of dynamic Range and it samples at 2.5 MSPS. It has a built in Finite Impulse Response (FIR) filter which limits f_{max} to 1 MHz. T_{sample} can now be calculated by

$$T_{sample} = \frac{2\beta R_{max}}{f_{max}c} \quad (2.13)$$

This gives that T_{sample} should be 1 ms, $N_{samples}$ is 2500 and S_r is 150 MHz per 1 ms. The range to the target is calculated by

$$R = \frac{fc}{2S_r} \quad (2.14)$$

This means that the difference frequency measured will increase by 1 kHz for every 1 m to the target. The value of $T_{sweep} - T_{sample}$ is chosen as 50 μ s. The frequency is therefore swept by 157.5 MHz in 1.05 ms.

The power to be transmitted is determined by the sensitivity of the ADC. The minimum power that the ADC can digitise is -100 dBm and it saturates at 0 dBm. The dynamic range of the radar needs to be at least 120 dB for it to cover the 1000:1 range specification. Variation in the RCS of the target can add another 40 dB, or more, to the required dynamic range. The required dynamic range of the system decreased by adding a SFC filter after the mixer. The power levels must be calculated in such a way that none of the amplifiers nor the mixer saturates.

Automatic gain control (AGC) needs some investigation, but the gain might be determined by the coupling between the antennas. If the AGC is added after the SFC filter it can be used to ensure that the biggest target present will have an amplitude equal to full scale on the ADC. This ensures that the entire dynamic range of the ADC can be used. In the absence of near targets this will enable the system to detect targets that are further away. In the presence of large, near targets it will prevent the ADC from being saturated.

2.2 Data Processing

2.2.1 Sampling and FFT

The data is captured using an ADC. This means that a discretised representation of the time domain data is generated. As the information that is of interest is in the frequency domain an FFT is taken.

It is not possible to calculate an FFT of a continuous signal, as there would be an infinite number of samples. The data is therefore divided into windows. These windows are chosen in such a way that 2500 ($N_{samples}$) samples are taken during the last 1 ms before the frequency of the DDS is reset.

2.2.2 Windowing

Windowing the data adds frequency components to the signal that need to be isolated from the frequencies that indicate the presence of targets. Adding an amplitude taper to the window will reduce the amplitude of these frequencies. Different amplitude tapers are shown in figure 2.5. The effect of the different tapers are shown in figures 2.6, 2.7, and 2.11 on page 22. The windows are calculated using one of the functions written for the simulations [9]. The simulation function is presented in section A.7 on page 89.

The amplitude taper means that a part of the signal is attenuated. This is seen, after the FFT, as an attenuation of the power reflected by a target. This can be seen in figure 2.11 on page 22, which shows simulated results using the different tapers.

Figure 2.6 shows the normalised frequency responses of the different windows. The widening of the main lobe and the suppression of the side lobe levels can be seen. The loss in amplitude due to the window can not be seen because of normalisation.

Figure 2.7 shows how a single target can look like many targets. The Blackman-Harris (B-H) window spreads the main lobe, reducing resolution, but the side lobes are -92 dB below the main lobe. The square window has a much sharper main lobe, but the side lobes are much higher, at 13 dB below the main lobe. The figure clearly shows that the B-H window masks the targets that are less than 4 m apart, but if the targets are more than 4 m apart then the square windows side lobes are more likely to mask the presence of targets.

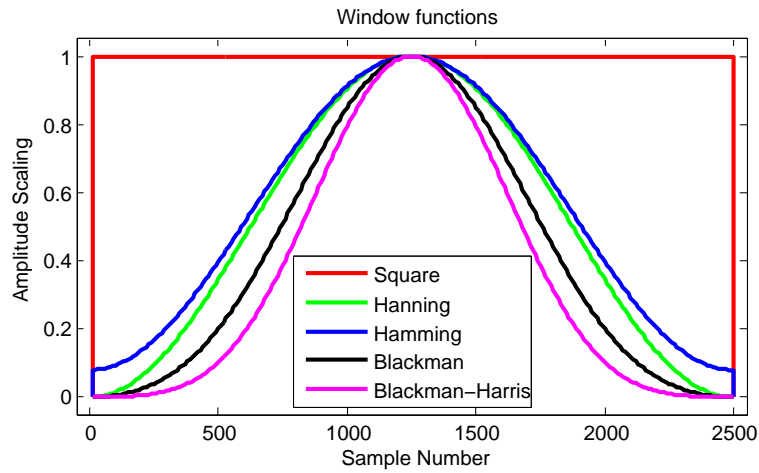


Figure 2.5: Windowing functions

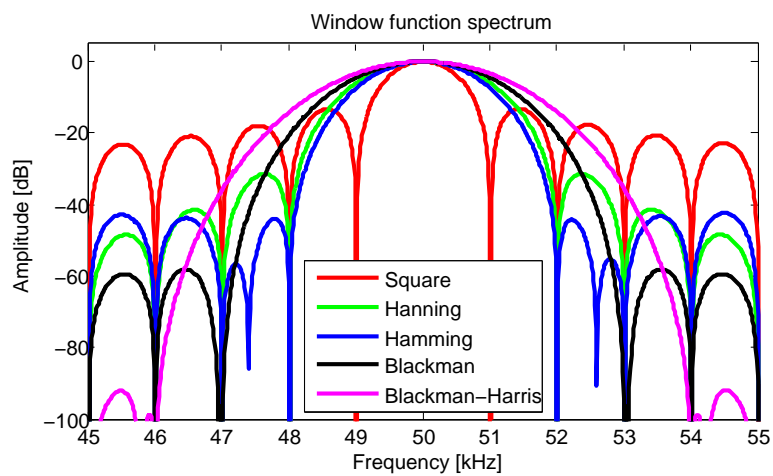


Figure 2.6: Windowing functions

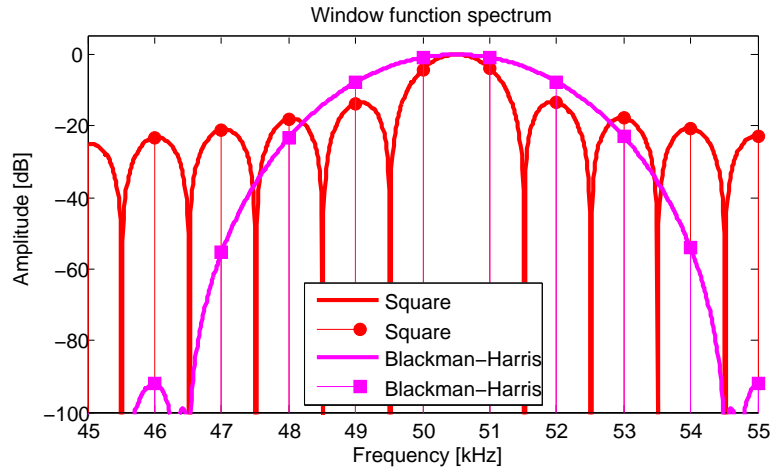


Figure 2.7: Effect of windowing functions on simulated radar

2.2.3 Sensitivity Frequency Control

The radar equation, Equation 2.15 provides a good understanding of the attenuation due to range. As the attenuation due to range is known, it can be removed mathematically. Adding a gain term (α) to the radar equation gives

$$P_r = \frac{P_t A_e G \sigma}{16\pi^2} \frac{\alpha}{R^4} \quad (2.15)$$

Where P_r is the transmit power, P_t is the received power, G is the antenna gain, A_e is the antenna effective aperture, σ is the RCS of the target and R is the range to the target. P_t , G , A_e , and σ are all constant for a given target. If P_r is to be kept constant α needs to be varied as the range changes.

In pulsed radar systems sensitivity time control (STC) is used. STC is implemented by sweeping the gain (α) of the receiver after the pulse has been transmitted. To keep the power after the receiver constant the $\frac{1}{R^4}$ component can be exactly cancelled if the receiver gain is swept at R^4 in time, this is assuming that the speed of propagation is constant.

FM-CW radar cannot use STC because of the continuous wave. In an FM-CW system the gain needs to be swept in the frequency domain, after the mixer. To implement SFC a filter can be used. The $\frac{1}{R^4}$ in power translates to an attenuation of 40 dB per decade. The SFC filter will therefore need to cut

off at 40 dB per decade. If the filter covers the entire band of the radar, this will give an attenuation of 120 dB at the frequency of the closest target. It is more practical to implement a filter that does not cover the entire band, but rather only attenuates the close targets as well as the coupling of the antennas.

As long as the frequency response of the filter is known, the SFC can be completed after sampling. The digital filter will need to implement the difference between the real filter and the ideal filter. This will result in all targets with the same RCS having the same amplitude signal, irrespective of range. The radar cross section (RCS) of the target can then be measured. In the measurements made with the practical system, see section 5.1.3 on page 62, the RCS of the targets are calculated using a different method. The amplitude of each target is calculated from the Radar Range equation and the SFC filter response where all the variables, except the RCS, are known. This method is used as it is easier to implement and is computationally less expensive.

If the SFC were to be implemented entirely in software it would not increase the dynamic range of the system, as this would still be limited by the sensitivity of the ADC. The SFC filter is added after the mixer, and so it does not help to prevent the receiver amplifiers or the mixer from saturating.

The filter is designed using a program 'Elsie', which is specifically designed for the design and analysis of RLC filters. The schematic for the filter is given in figure 2.8. The component values are given in table 2-I.

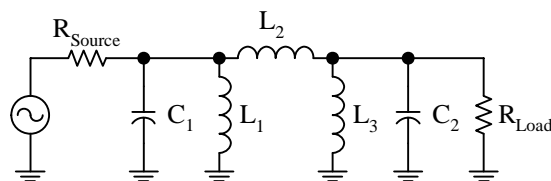


Figure 2.8: SFC Schematic

The simulated results of the SFC filter is plotted in Figure 2.9. The filter is built and measured, see section 3.4.5 on page 41. A radar was also simulated with ideal SFC filters, as discussed in section 2.3.1 on page 21

Table 2-I: Filter Component Values

Component	Value
L1	$100\mu H$
L2	$6.8\mu H$
L3	$100\mu H$
C1	$6.6nF$
C2	$6.6nF$

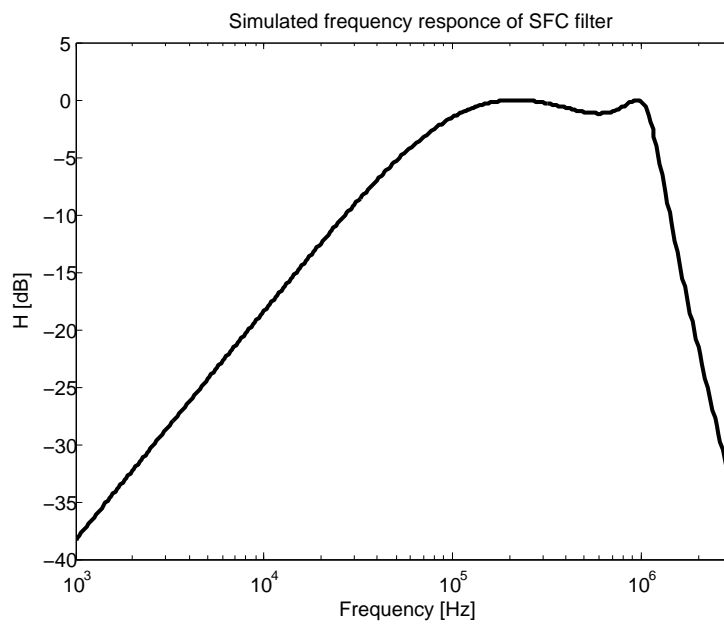


Figure 2.9: Frequency response of SFC filter

2.3 Simulations

The system shown in figure 2.1 is verified by simulation.

It has been shown, in section 2.1, that the centre frequency of the system does not affect the output of the Radar. It is therefore decided to simulate the system at the base band of the DDS. The results obtained in the simulations, where the frequency is swept from 100 MHz to 275.5 MHz, will also be valid for the practical system where the frequency is swept from 5.75 GHz to 5.9GHz. The simulated output of the DDS is ‘transmitted’ at 1 Giga samples per second (GSPS) as it is generated. The simulations therefore carry the information at 1 GSPS until it is ‘sampled’.

Figure 2.10 shows the block diagram of the simulated radar. It differs slightly from Figure 2.1, on page 5, in that the antennas and the propagation to the target is lumped into one block.

Each function is represented as one block. A list of the input arguments to the function is given in the middle of the block and the outputs are given at the bottom. The discussion that follows is a brief summary of the functions and how they fit into the system. The complete functions, including a description on how to use them, are shown in Appendix A.

The DDS function generates the frequency sweep signal. The frequency is stepped from the start frequency to the stop frequency in a time of *Ramp Length*, the frequency is stepped at a specified time, *Step Time*. The other input parameters set the *Start Phase* and the *Modulation Type*. For the purposes of debugging, the *Amplitude* or *Phase* of the output can be given as the output. If the phase is differentiated, the output frequency can be plotted as a function of time.

The DDS function works on the same principle as the DDS, see section 3.1. It generates the output of the phase accumulator, which is then converted to an instantaneous amplitude. The DDS uses a lookup table (LUT) to find the 10-bit amplitude that is given to the digital to analog converter (DAC).

The DDS function gives the output at the voltage of the specified output power. This is done to simplify the simulations. In reality the DDS gives a fixed power output, which is then amplified to the correct power levels. The phase samples are at 1 ns intervals as they would be from the DDS.

Another function was written that gives the output of a pure linear

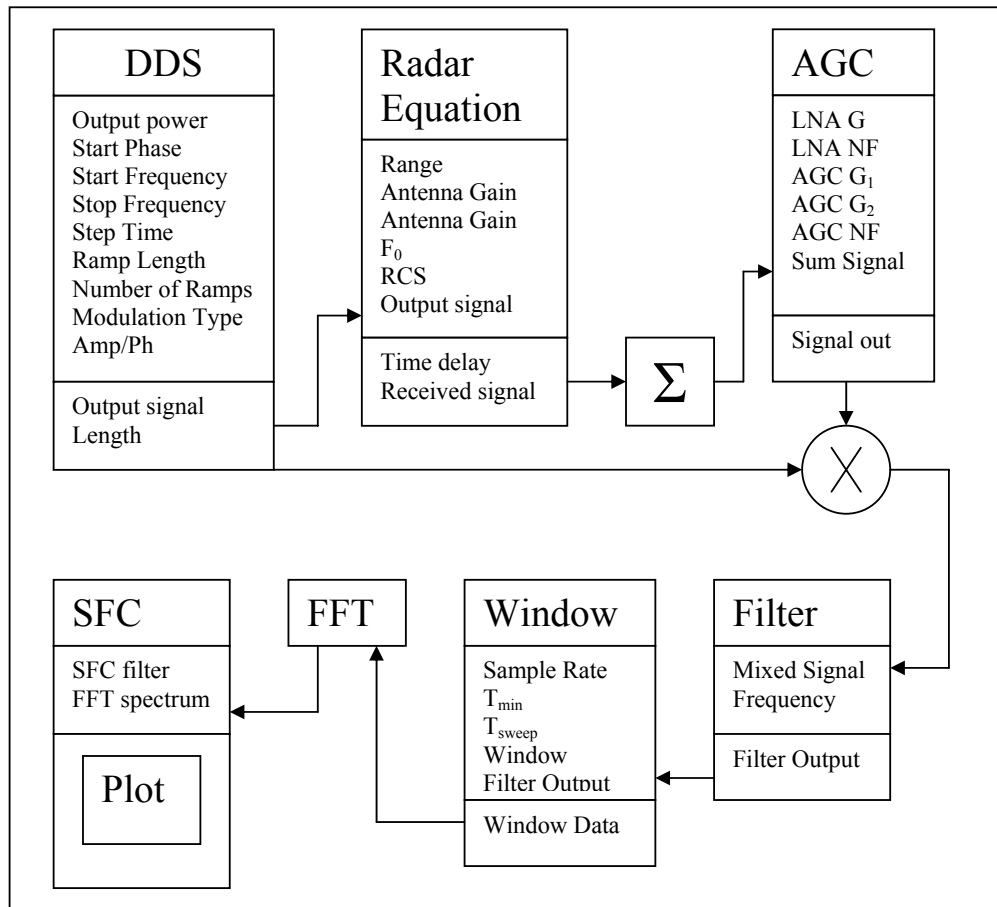


Figure 2.10: Block diagram for simulations

frequency sweep. It accepts the same inputs as the DDS function, step time is, however, ignored. This function is used for comparison of the DDS output and the linear sweep. It is much faster than the DDS function and is therefore used for most of the simulations.

The radar equation, equation 2.15, is implemented in a function that calculates the attenuation due to the propagation as well as adding a time delay to the signal. All of the variables in the radar equation are required as inputs. The effective aperture area (A_e) of the receive antenna is calculated from the antenna gain (G) and the centre frequency (F_0). This function only works for single targets but can be used for multiple targets if it is called multiple times and the results are added. The radar equation function does

not add any environmental noise to the signal.

A function was written to simulate the effect of the AGC. The function implements two amplifiers, the first having a fixed gain, the second a variable gain. This is used to simulate a system that has a low noise amplifier (LNA) followed by AGC. If the second amplifier is used as a fixed gain amplifier, the minimum and maximum gains are set to the same value. Each of the amplifiers can add a certain amount of noise. The noise that each of the amplifiers add is calculated from the noise figure of the amplifier [10]. The simulation results are not included as it is not included in the practical system and more work needs to be done before any useful conclusions can be made.

After the signal is amplified, it is mixed with the output of the DDS. The mixer is implemented as the multiplication of the two signals. This is an ideal mixer, and the non-linearity of the mixer is not considered.

A single pole low pass filter was implemented to separate the sum and difference frequencies. The impulse response of the system, given by equation 2.16, is convoluted with the unfiltered input. The 3 dB cut-off frequency is given as an input. The impulse response of the filter is considered to be negligible after 5 time constants 5τ .

$$h = \frac{1}{\tau} e^{-\frac{t}{\tau}} \quad (2.16)$$

The simulated system is discrete, but up to this point it works with the 1 GSPS that is generated by the DDS function. The window function reduces the number of samples to that which will be sampled by the ADC. The sampling rate is given as an input, as are the beginning and the end time of the sampling window. An amplitude taper is then added to the sampled data. The window is chosen with another input, as in table 2-II

The frequency spectrum of the sampled data is then calculated using MATLAB's FFT function. The SFC filter can be added using the SFC function, before the spectrum is plotted.

All of the simulations were done with stationary targets, but the DDS function can be used twice in order to simulate moving targets. To simulate the Radar with a moving target the signal needs to be delayed and a doppler shift needs to be added. By using the DDS function twice, two frequency sweeps can be generated where one is equal to the other plus a doppler shift.

Table 2-II: Window Function Taper Selection

Window	#	side lobes	beam width
Square	0	13	2
Hamming	1	45	4
Hanning	2	27	4
Blackman	3	58	6
Blackman-Harris	4	92	8

The doppler shifted signal is then passed to the Radar Equation function that delays and attenuates the signal. This doppler shifted, delayed signal is then multiplied by the original signal. The rest of the Radar is then simulated in the same way as for stationary targets.

2.3.1 Simulation Results

The simulated system sweeps the frequency from 100 to 257.5 MHz in 1.05 ms. It transmits 0 dBm of power, and the antennas have a gain of 10 dB. There are 5 or 10 targets, each with a RCS of $1 m^2$, placed at 50 m intervals.

All the simulation results that are shown were run using the MATLAB functions. For the 1 050 000 sample simulations the time per simulation is approx 3h30 with the DDS, compared to 3 min with DDSapp. After running the simulations the DDS function was rewritten using C⁺⁺. The C⁺⁺ function simulates the DDS and writes an output file in 2,5 seconds. If further simulation is necessary, rewriting all of the functions in C⁺⁺ would save a significant amount of time.

Figure 2.11 shows the simulated results of the radar with different windowing functions. An apparent loss in power, due to the window, of almost 10 dB can be seen between the square and B-H windows. For the square window the first side lobe is 13 dB below the main lobe, and the smallest side lobes, furthest from the targets are 37 dB below the main lobe. The B-H window has a first side lobe level of 92 dB below the main lobe but the highest side lobes are 44 dB below the main lobe. There is therefore an improvement of 7 dB in the ratio between the main lobe and the biggest side lobe. The apparent loss in power is therefore acceptable, as the side lobes are suppressed

more than the signal is attenuated.

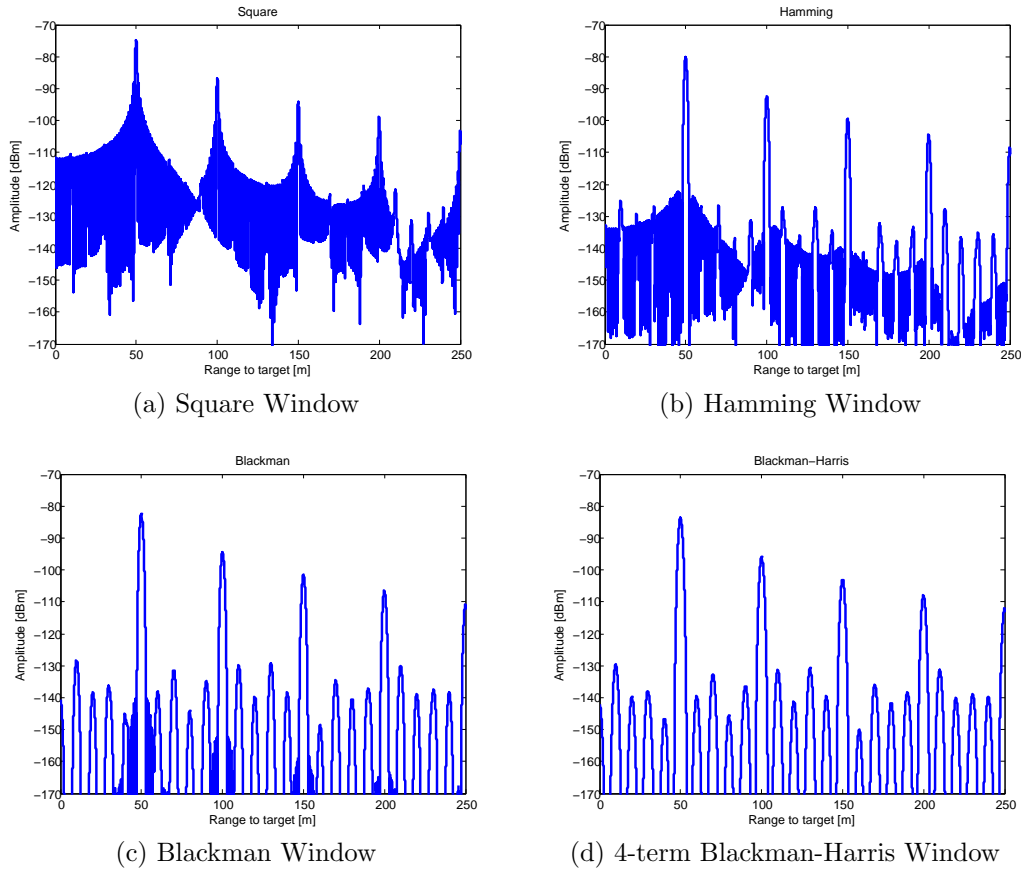


Figure 2.11: Simulations with different windowing functions

Figure 2.12 shows the output frequency spectrum of the simulated radar. The known positions of the targets are also plotted. The furthest target, at 500 m, is only 3 dB above the side lobes of the previous targets. One would expect that the amplitude of the targets would decrease with increasing range. The target at 450 m is, however, bigger than the target at 400 m. This is as a result of the targets adding in phase with the side-bands of the closer targets.

The effect of the SFC filter was also simulated. Figure 2.13 on page 24 shows the results without SFC, with 20 dB/decade SFC and with 40dB/decade SFC. When SFC of 40 dB/decade is implemented, all targets with the same size will be of the same amplitude. SFC can also be implemented digitally,

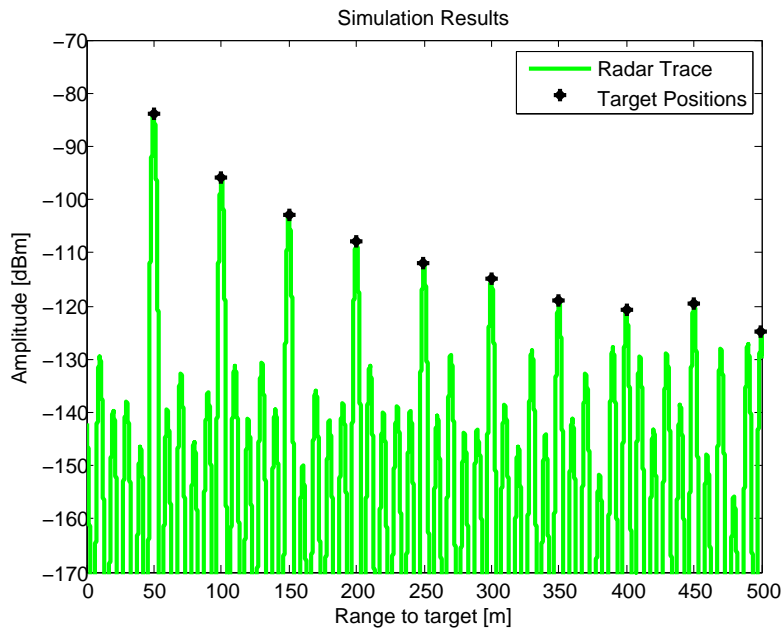


Figure 2.12: Simulation results without noise

after the FFT. The non-ideal response of the SFC filter, see figure 3.8 on page 42, can be compensated for.

The working of a DDS is given in section 3.1 on page 31. A DDS does not give linear FM, but is a very good stepped approximation, the effect on this was also simulated to determine its effect. In these simulations only 5 targets are used. The radar is simulated with the DDS output and with a perfect linear frequency sweep. The DDS generates a stepped frequency, with 1200 Hz steps every 8 ns, which gives a total of 150 MHz in 1 ms. The results of the two simulations are plotted in figure 2.14 on page 24. There is no noticeable difference at the targets, but some of the side lobe levels are higher when the DDS is used. To keep these side lobes to a minimum the steps should be kept as small as possible and the step time should be as short as possible.

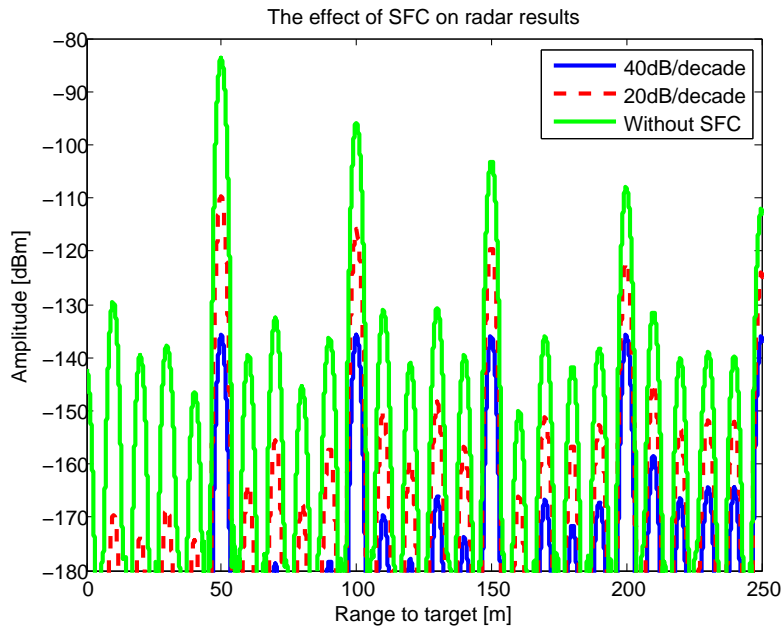


Figure 2.13: The effect of Sensitivity Frequency Control

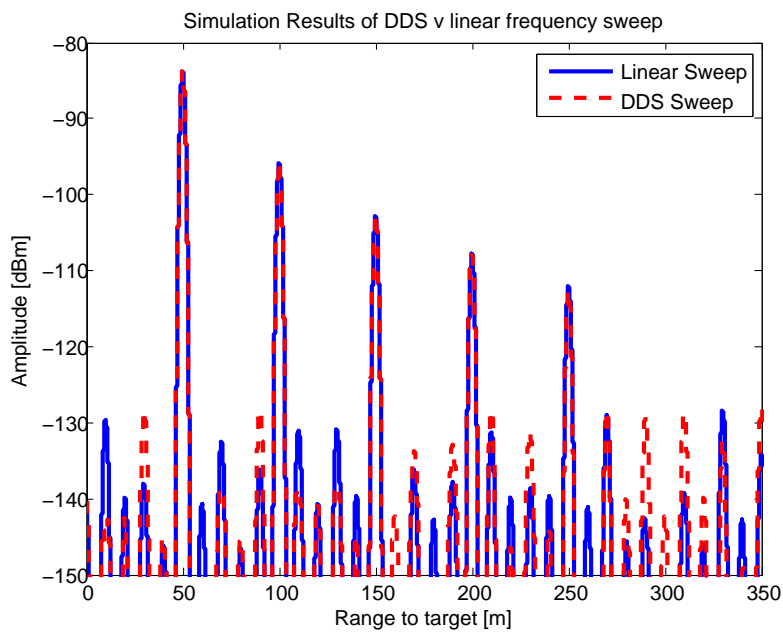


Figure 2.14: Plot of simulation results comparing the true linear frequency sweep v the DDS output signal

2.3.2 Simulation Results With Noise

Phase noise of the local oscillator (LO) is discussed in section 3.3.1, on page 34. The only noise that is added to the simulation is calculated from the amplifiers' noise figure (F), as given in the data sheets. The noise contribution from the mixing process is not included. The definition of noise figure is given by equation 2.17 [10].

$$F = \frac{S_i/N_i}{S_o/N_o} \quad (2.17)$$

$$F = \frac{S_i N_o}{N_i S_o} = \frac{S_i N_o}{N_i G S_i} \quad (2.18)$$

It is assumed that N_i is the noise from a matched resistor at $T_0 = 290K$, or $N_i = kT_0B$. If it is assumed that the noise from the antenna is the same as that from a matched resistor, the noise that is added at the output of the amplifier is

$$N_0 = FGkT_0B \quad (2.19)$$

The system is simulated with noise added and the results are plotted in figure 2.15. The noise that has been added is that of a single amplifier, the Hittite HMC318MS8G, with 9 dB of gain and a noise figure of 2.5 dB, the bandwidth is 150 MHz. The noise floor is higher than the side lobes from the sampling. As a result of this many of the targets cannot be seen. Of the ten targets in this simulation only the first one can be found with certainty, as it is 15 dB above the noise floor. There are targets that will be missed and the probability of a false target is increased.

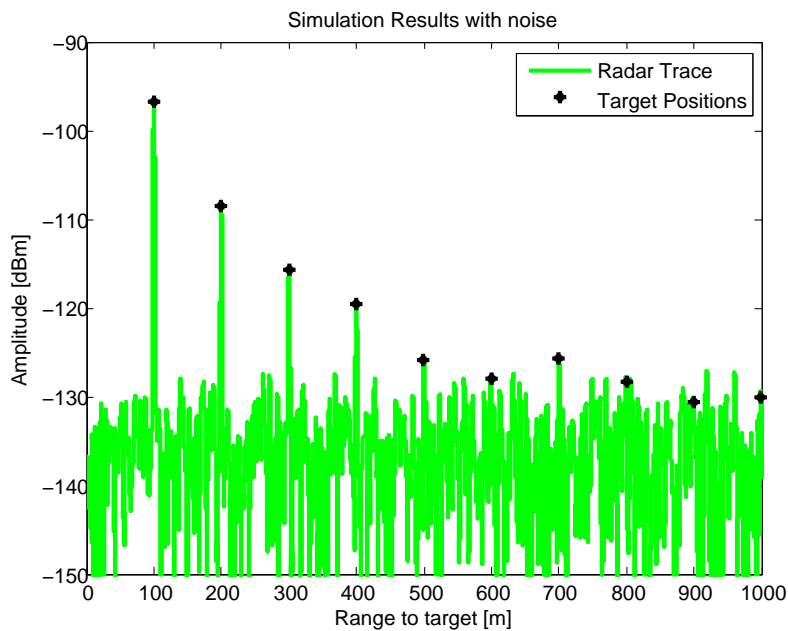


Figure 2.15: Simulation results with noise

2.4 Experimental Proof of Concept

2.4.1 Setup

An experimental system was set-up using general lab test equipment. The block diagram for the system is shown in figure 2.16. The DDS is replaced by two signal generators. The first generates a saw-tooth, that is used as the input to the frequency modulator of the second. A PLL is used to multiply the frequency from the signal generator, as the frequency modulator has limited bandwidth. The system is shown figure 2.17.

A digital oscilloscope, which samples at 500 kSPS, is used for the ADC. The radar measures across the lab to the VNA on the workbench shown in figure 2.18. The distance from the radar to the chairs at the network analyser is approximately 5 m, and the distance to the wall is 6 m.

The length of the cables used give time delays that are similar to the time delay from close in targets. Since the measurements are taken across the width of a lab that is no more than a couple of meters wide, all targets are close. The effect of the long cables is reduced by the fact that both the transmitted

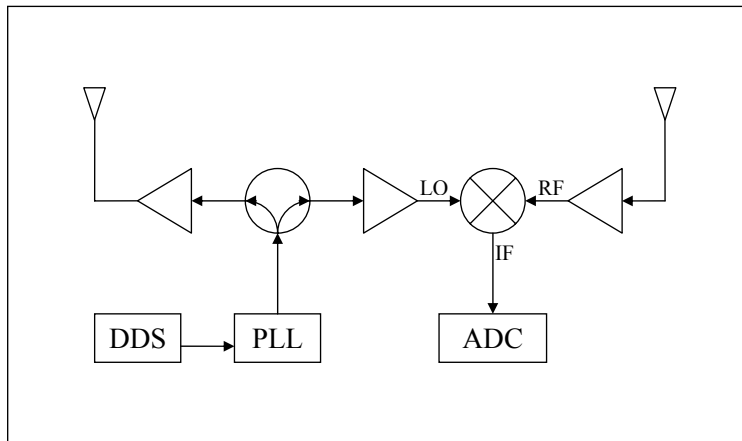


Figure 2.16: Block diagram as used for the experimental proof of concept

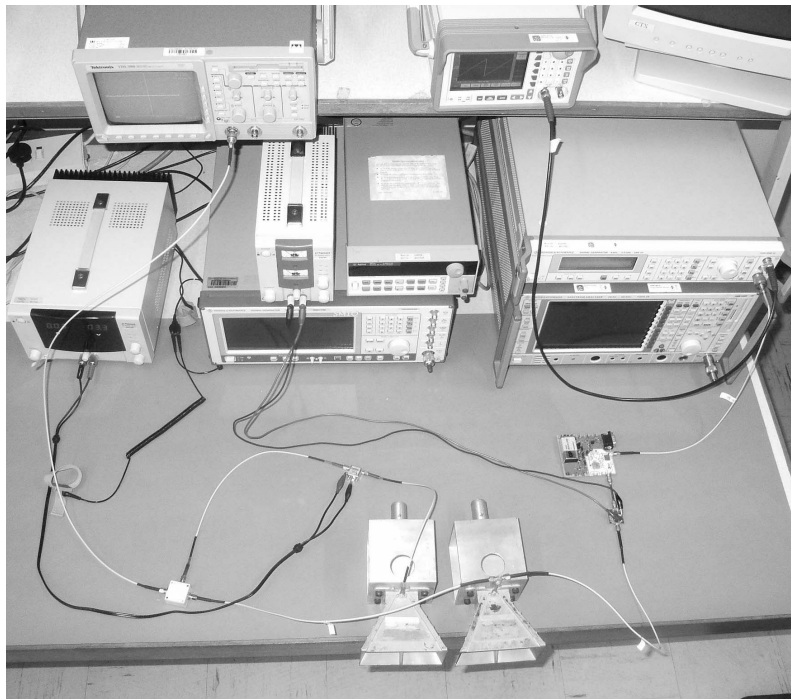


Figure 2.17: Photo of proof of concept experiment



Figure 2.18: Photo of proof of concept Target

and received signals have a time delay before the mixer. The antennas have a band width from 2 to 18 GHz, which means that there is out of band noise that will be received and added to the system. This noise could be removed by adding a band-pass filter after the antenna. The oscilloscope has a low pass filter (20 MHz) so there is no need to add an external filter to remove the sum frequency that will be seen at 11.5 - 11.8 GHz.

2.4.2 Results

The measured results are plotted in figure 2.19. The plot shows three results. The first is a measurement of the environmental clutter, the second a measurement with a target at a distance of 5 m. The third trace is calculated by subtracting the clutter from the target measurement, before taking the FFT. A radar that uses clutter subtraction is commonly referred to as a moving target indicator (MTI).

Antenna coupling can be seen clearly, appearing as a target at 1 m. This target disappears completely when clutter subtraction is applied.

In the measurement with the target, there are 2 targets, at 3.5 m and 4.5 m respectively, that can clearly be seen above the clutter. When the clutter is

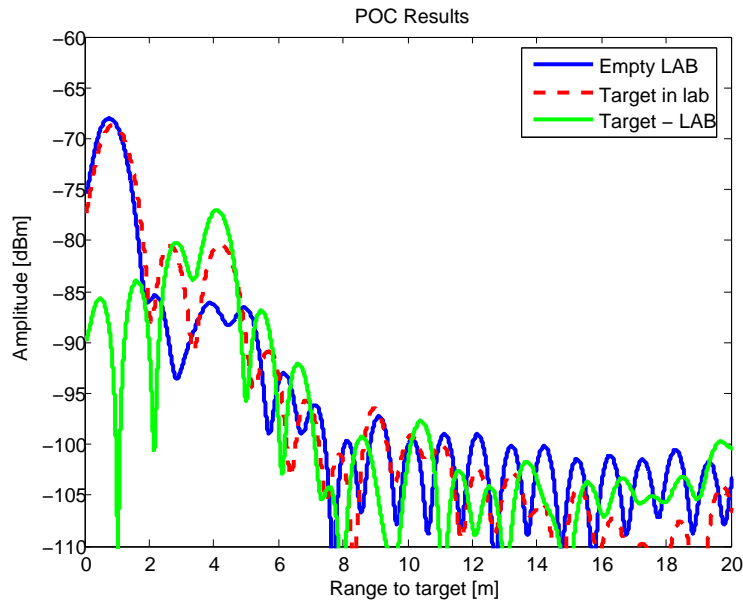


Figure 2.19: Measurement Results

subtracted the target at 4.5 m increases by 4 dB. There then appears to be only one target at 4.5 m with side lobes decaying to either side.

The reason for the inaccuracy of the position of the target is the difficulty of determining the exact frequency swept by the signal generators FM modulation.

2.5 Conclusion

The parameters required for an FM-CW radar, presented in table 2-III, were calculated mathematically, and simulated to verify. A practical system is also built as a practical proof of concept.

It is calculated that to meet the specification of a range resolution of 1 m, the system needs to have a bandwidth of 150 MHz, or more. This needs to be swept in 1 ms in order to meet the specified range of the system. The values of bandwidth and sweep-time are verified by simulation. These values are used in a practical system and the results are promising.

Table 2-III: Parameters for FM-CW Radar

Parameter	GPR	Pedestrian
Block diagram	Figure 2.1	Figure 2.16
β	300 MHz	150 MHz
T_{sample}	1 ms	1 ms
f_{sample}	2.5 MSPS	2.5 MSPS
N_{sample}	2500	2500
Δf	1 kHz	1 kHz
f_{min}	1	1
f_{max}	1000	1000
τ_{max}	3.3 μ s	6.7 μ s

Chapter 3

Sub-System Components

In this chapter the block diagram, designed in chapter 2, is discussed in more detail. The cost of the components are given in chapter 6. The working of each block is discussed both as an entity on its own and as part of the system. The influence of each block on the system performance is also presented. The main focus is on the working of the blocks as they are used in this system. The design of the antennas is presented in chapter 4.

3.1 Direct Digital Synthesizer

The DDS is an important component of this radar. It is the component that enables good linearity of the frequency sweep. The linearity of the frequency sweep is an important aspect of FM-CW radars. Without the linear frequency sweep the range data cannot be extracted accurately.

A DDS works on the principle of a phase accumulator. The user provides a starting phase and frequency. The frequency is used to calculate the phase increment of the output signal in one period of the input clock. The phase accumulator then adds this phase increment to the previous phase value once per input clock cycle. A LUT is then used to transform the phase to an immediate amplitude. A DAC then provides the analogue output of the DDS.

For this project the Analog devices AD9858 is used. It has a 1 GSPS output rate and can be used to give a sinusoidal output with a frequency of up to 400 MHz. It also has a frequency accumulator in addition to the phase accumulator. The frequency accumulator is programmed so that the frequency

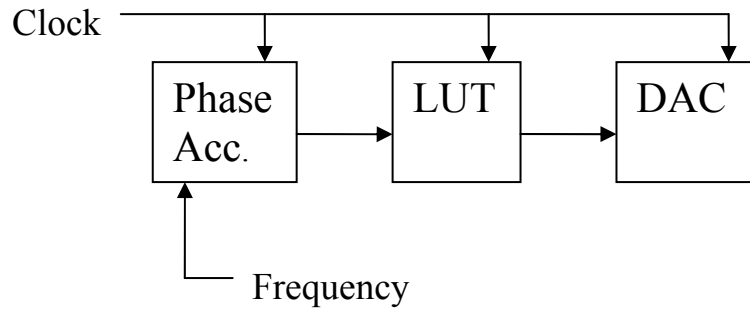


Figure 3.1: Block diagram of DDS

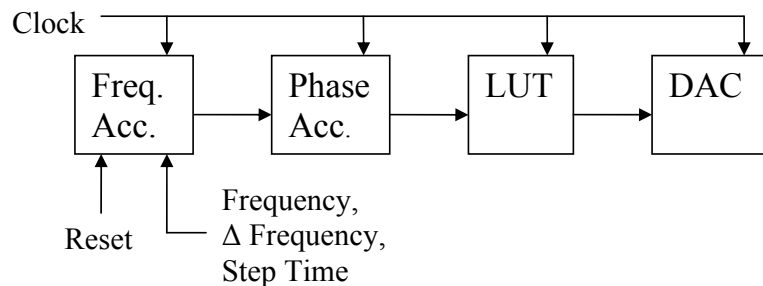


Figure 3.2: Block diagram of DDS with frequency accumulator

is incremented by a specified value at a specified rate. The minimum time between frequency increments is 8 ns. In effect the frequency of the output is incremented in steps. This stepped frequency is very close to a linear sweep, especially if the time and the frequency increments are small. The effect of the stepped frequency was simulated and the results show that it does not affect the system performance. The results of this simulation are shown in figure 2.14. At the end of the sweep the frequency is reset by an external signal. In the final system this is generated by a field programmable gate array (FPGA).

3.2 Phase Locked Loop

A PLL is a feedback system that is used to create an output signal that has the same frequency as a reference signal. Figure 3.3 shows a block diagram describing a generic PLL. The phase of the output signal is compared to

the reference signal. If the phase difference changes, the input voltage of the voltage controlled oscillator (VCO) changes which, in turn changes the output frequency of the VCO. This stabilises the phase difference. If the phase difference between the two signals is constant, the frequencies are the same.

A frequency divider can be added to the feedback path. If the frequency divider divides the frequency by N , then the output frequency must be N times the input frequency in order for the frequencies at the input of the phase comparator to be equal. In this configuration the PLL is used as a frequency multiplier.

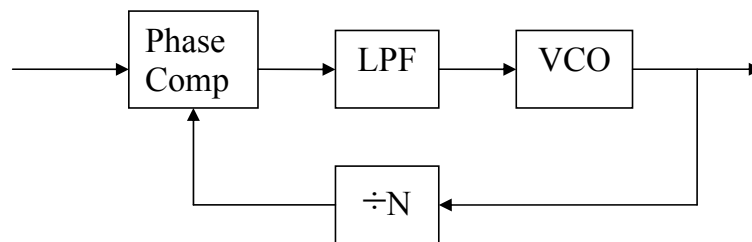


Figure 3.3: Block diagram of PLL

For the pedestrian radar a PLL is used to multiply the frequency of the DDS to 5.8 GHz. The low pass filter at the input of the VCO limits the rate at which the frequency can change, and so it smooths the frequency steps produced by the DDS.

The PLL that is used in the practical system is the ADF4106 Evaluation board from Analog Devices. It uses a Z-Communications V940ME03-LF VCO. This VCO has a tuning bandwidth of 250 MHz, this is further limited by the PLL to 150 MHz. To maintain the linearity of the sweep generated by the DDS N needs to be kept low but the phase comparator has a maximum input frequency of 300 MHz, so N has to be 20 or bigger. The PLL is therefore used to multiply the frequency by 20, and the DDS frequency is only swept from 287.5 MHz to 295 MHz. The PLL has a loop bandwidth of 50 kHz.

The use of a mixer should also be considered, where the DDS signal is mixed with a signal of constant frequency. If this method is used then the

full bandwidth of the DDS might be used, in which case a frequency sweep of 300 MHz can be achieved. The image frequency that results from mixing will have to be removed by filtering. If the DDS sweep of 50 MHz to 350 MHz is mixed with a signal at 5.75 GHz, the resulting signal will have a frequency sweep from 5.8 GHz to 6.1 GHz, with an image signal that will sweep from 5.7 GHz to 5.4 GHz. The image frequency will have to be removed by filtering.

The VCO of the PLL will have certain phase noise and frequency stability characteristics that will add to any phase noise or frequency instability from the DDS that has been multiplied, lowering the system performance.

In the GPR the DDS is the only source of phase noise, while in the pedestrian radar the DDS and PLL both contribute to the phase noise. The phase noise of the DDS is multiplied by 20 (290 to 5800 MHz). To minimize the system phase noise the VCO must have low phase noise, but the phase noise of the DDS must be 20 times lower, otherwise it will dominate the system Phase noise [11].

3.3 Local Oscillator

A low phase-noise LO is required for the DDS, as it will effect the phase noise of the entire system. A 1 GHz ceramic oscillator is used and compared to a reference oscillator [12].

3.3.1 Phase noise

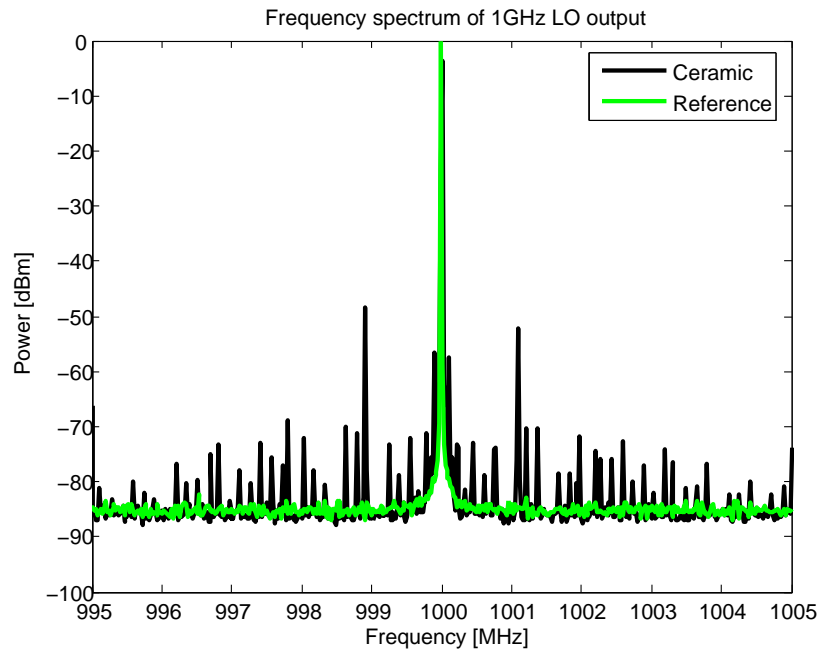
Phase noise is a problem in FM-CW radar. As high frequencies are mixed down to very low frequencies over an extended period of time, the sensitivity to phase noise is increased [13; 14]. Phase noise can be contributed by the DDS or the PLL's VCO.

The spectrum of the LO and the DDS are measured and compared to measurements made using a low phase noise reference oscillator [12]. The DDS is programmed to give an output signal with a frequency of 290 MHz. The spectra of the oscillators are shown in Figure 3.4a. The measurements were made on a spectrum analyser with a resolution bandwidth of 10 HZ. The spectra of the 290 MHz DDS signals, using the two LOs, are shown in Figure

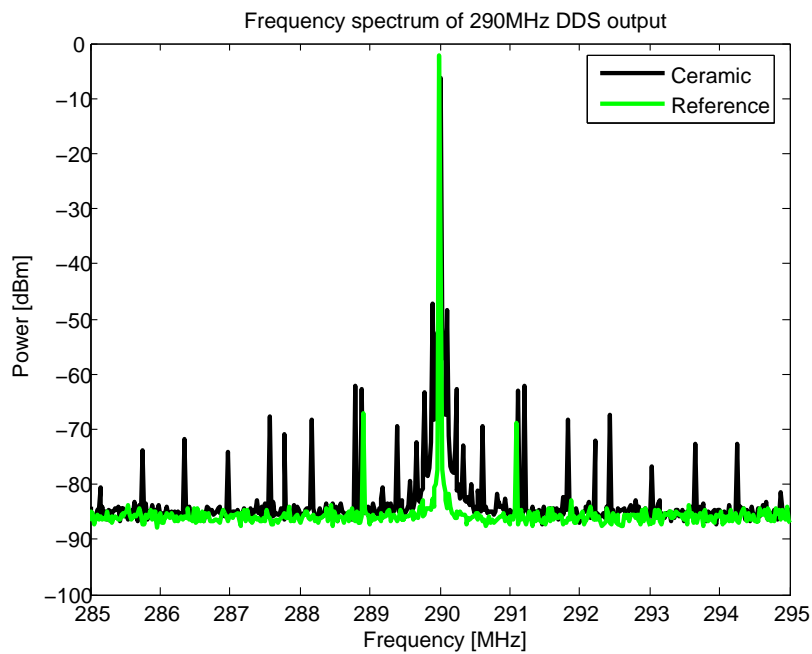
3.4a. The DDS is used to divide the LO frequency to the required frequency, and in so doing also averages the phase noise of the LO

The spectral content that is of concern is within 1 MHz of the centre frequency. When this signal is multiplied with a time delay of itself, the frequency content of these frequency components will be mixed to below 1 MHz. The radar will 'see' any frequency below 1 MHz as a target. The phase noise will cause a rise in the noise floor and phantom targets can appear. This investigation of the LO's phase noise is not sufficient to describe the effect of phase noise on the entire system. There are many more factors that will affect the phase noise of the system, like the phase noise of the PLL's VCO, and the fact that there is noise cancellation due to the fact that the phase noise of the transmitted and received signals are similar. A detailed investigation needs to be done to determine the effect of these factors on the system performance.

There is AM distortion on the DDS output, this is seen as peaks in the spectrum at 1.1 MHz either side of the desired signal. In the radar where a PLL is used this is not a problem, as the AM does not affect the PLL, the PLL is only affected by the phase of the incoming signal. The modulation is as a result of the 1.1 MHz switching frequency of the LT1940 voltage regulator, see section 3.4.1. This is confirmed by the fact that the AM distortion is not seen on the reference oscillator which runs off an external voltage source.



(a) LO Spectrum



(b) DDS Spectrum

Figure 3.4: LO and DDS Spectra

3.4 Analog

3.4.1 Voltage regulators

Switch mode regulators are used to supply the different voltage levels required by the different components of the pedestrian radar. The GPR system only requires two voltage levels, a bench power-supply is therefore used. In section 5.3 on page 69 it is shown that the noise on the voltage regulators have an adverse effect on the system performance.

An LT1940, a dual switch mode regulator from Linear Technologies, is used to provide 3.3 V for the DDS and LO. It also gives 7.5V for the ADC, it switches at 1,1 MHz. A Traco DC/DC converter is used to provide 5 V for the PLL, as well as some amplifiers. The 5 V is also regulated by linear regulators (LM 317) to provide 3 V for the rest of the amplifiers and later to provide 3.3 V for the LO.

3.4.2 Amplifier

Various amplifiers are used in this project, all of which were measured. An example of one of the measurements is given in figure 3.5. A summary of all the measurements is given in Table 3-I. It shows the minimum f_l and maximum f_h frequency as well as in which of the two systems the amplifier is used.

Table 3-I: Measured Amplifier Specifications

Amplifier	f_l [MHz]	f_h [MHz]	Gain [dB]	Radar
HMC318	5000	6000	11	Pedestrian
HMC415	5000	6000	20	Pedestrian
ZX60-5916M	1500	6000	13	Pedestrian
HMC580	15	850	22	GPR
HMC589	20	4000	22	GPR
AD8138	0	1	0	Both

Many of the amplifiers used have much more bandwidth than the system requires, which adds unwanted noise. This noise can be reduced by the addition of a band pass filter after the receive antenna.

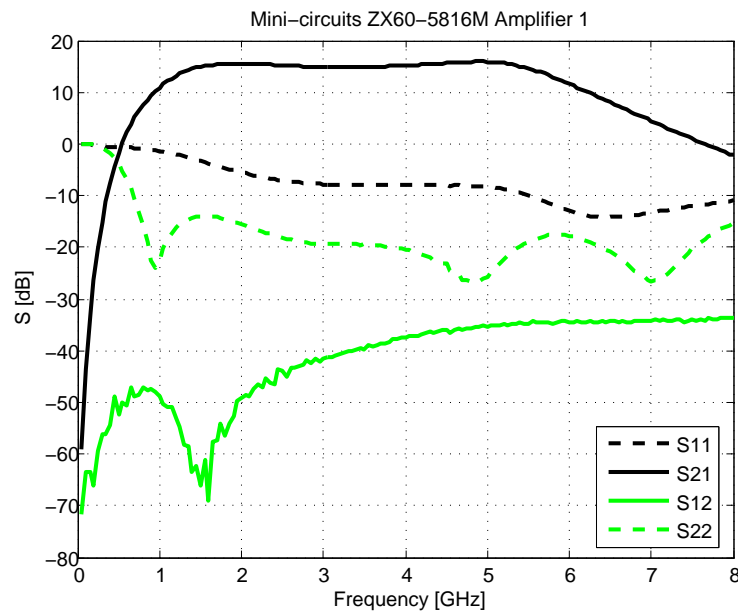


Figure 3.5: Measured S-parameters of Mini-Circuits amplifier

The fact that the amplifier gain is not flat over the frequency band that is used means that there will be some AM added to the signal. As the frequency of the output signal increases the gain of the amplifiers decrease, this will lead to the amplitude of the signal to decrease in time until the frequency is reset to the original value. This needs to be studied in more detail to see if this effect can be removed, possibly by using an AGC, or even if it can be used if more advanced processing of the data is used.

3.4.3 Mixer

The DDS has a built in Gilbert cell mixer that is used for the GPR. This mixer is the same as the AD8343 mixer from Analog Devices. For the pedestrian radar, a Mini-Circuits ZX05-C60 balanced diode mixer is used. Table 3-II gives some of the important characteristics of the ZX05-C60 mixer. The LO-IF (Intermediate Frequency) and the LO-RF (Radio Frequency) Isolation as well as the conversion loss is given.

The DDS Gilbert cell mixer requires an LO power of -10 dBm and has a conversion gain of 3.5 dB. The pedestrian radar's mixer requires 10 dBm of LO

Table 3-II: Mixer characteristics

Frequency	Conversion loss	Isolation	
		LO-IF	LO-RF
5700	6.0	15.7	23.7
5750	6.2	15.2	23.1
5800	6.4	15.1	22.6
5850	6.4	14.9	22.9
5900	6.5	12.5	23.5

power and has a conversion loss of 6.4 dB. The additional power required for the mixer in the pedestrian radar an additional amplifier. The GPR requires about 10 dB less Rx power to result in the same power at the output of the mixer.

3.4.4 Splitter

The generated waveform needs to be split into two parts, one to drive the LO of the mixer and the other to be transmitted. Both splitters that are used were measured, but only the results from the pedestrian radar is plotted. Figure 3.6 shows that the input power at port 3 is split equally between ports 1 and 2.

The pedestrian radar uses the ZX10-2-71 and the GPR the ZFSC-2-1. Both are from mini-circuits and have a maximum input power as splitter of 30 dBm.

An important factor of the power divider is that the time delay of the signals to the two output ports should be the equal. As in figure 3.6, both splitters were measured, but only one is plotted in figure 3.7. The phase delay is the same to the 2 output ports. The linear increase in phase delay, with frequency, indicates that the time delay is constant.

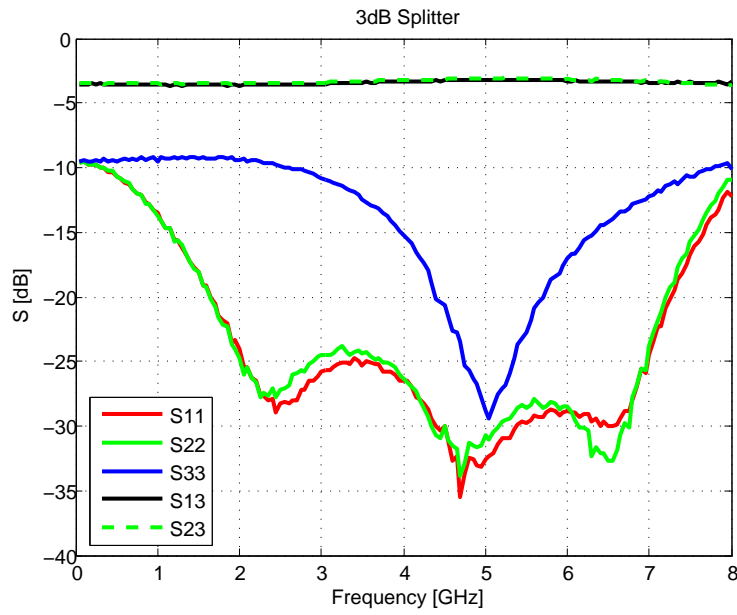


Figure 3.6: Splitter Measurements - Magnitude

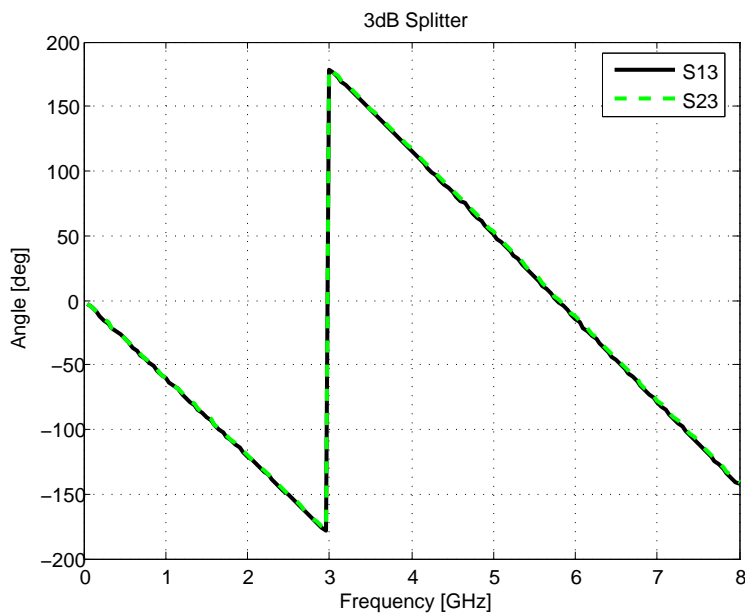


Figure 3.7: Splitter Measurements - Phase

3.4.5 Filters

Because of the wide bandwidth of the amplifiers there is a lot of out of band noise in the system that could be removed by the addition of RF selection filters. This is especially true in the case of the pedestrian radar. In the GPR system there are harmonics from the DAC that could be removed by the use of a low pass filter. The antennas are narrow band, which means that only the noise in that band will be received by the system. This means that RF selection filters would not decrease the noise by as much as they would with wide band antennas. The improvement could still, however, be notable.

A filter is also used for the SFC, see section 2.2.3 on page 15. The amplitude response of the SFC filter was both simulated and measured. The results are plotted in figure 3.8. Above 10 kHz the measured and simulated results are within 1 dB of each other, but at lower frequency the measured filter does not attenuate as much as the simulated filter. The reason for this deviation at low frequency is the resistance of the inductors. The 6.8 μH and 100 μH have series resistances of 1 and 4 Ω respectively. This is not seen at higher frequencies as the reactance is then bigger than the resistance. At 10 kHz the reactances are 0.43 and 6.2 $\text{j}\Omega$, respectively.

The SFC filter is built on a board that also converts single ended signal to differential, by means of an amplifier, for the ADC. The measured filter response is plotted for both the outputs of the differential signal.

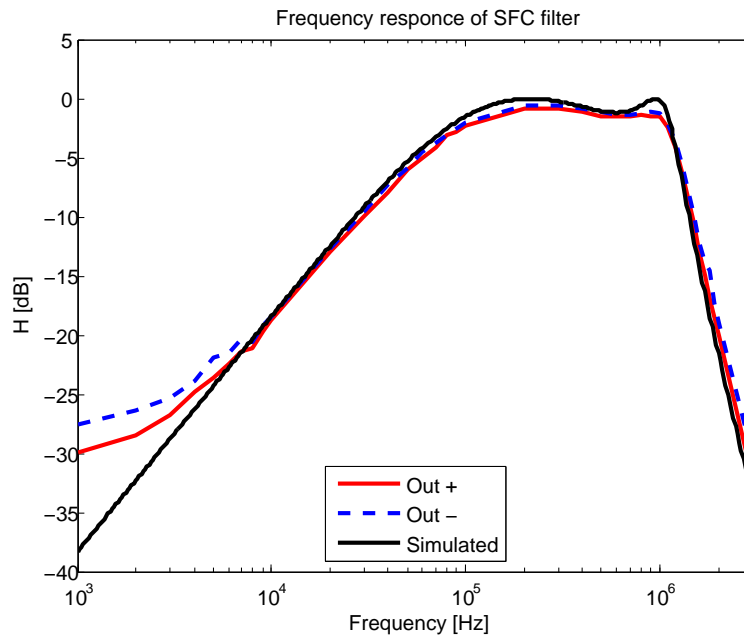


Figure 3.8: Filter Measurements

3.5 ADC

An Analog Devices AD7760 Σ - Δ ADC that is capable of giving 22-bit data at 2.5 MSPS is used. Σ - Δ ADCs generate a single bit sample at a higher frequency. This passes through a digital filter to generate the 22 bit samples [15]. The ADC incorporates a digital low pass FIR filter that has a 1 MHz cut-off frequency. This corresponds to 1000m of range for the pedestrian radar.

3.6 Conclusion

The components required for the implementation of both radar systems have been discussed. Many commercially available components exist that can be used in this system. Components that will satisfy the system requirements have been chosen. An effort was made not to use highly specialised, expensive, components, readily available components were rather chosen where possible.

Chapter 4

Antenna design

This chapter discusses the design and measurement of a patch array. Two other antennas that are used in the project are also mentioned. These were used, but they were not designed. The design of tri-hedral corner reflectors for test targets are also presented.

The layout of this chapter follows the method for designing the patch array, which was:

- Design of a single patch using Munson's equations, and compensate for the height of the patch [16].
- The patches were then placed in an array, and the effect of the coupling removed.
- Feed network with lumped element termination was designed with the correct spacing for the array.
- The patches and the feed network were then connected, and the feed pins designed. The layout of the antenna is shown in Figure 4.1. The ground has been removed for clarity.
- The antenna was then constructed and measured for comparison to the simulated results.

The patch antennas were simulated in *CST Microwave Studio*. The patch antennas were built and measured in an anechoic chamber before being used as a part of the radar system.

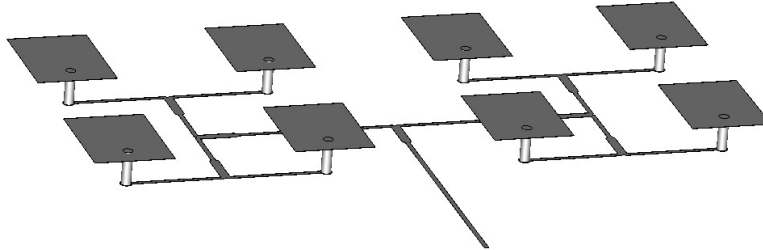


Figure 4.1: Antenna geometry showing feed network.

4.1 Patch

The patches were designed to be made with 3 layers of dielectric. The feed and the ground are etched on either side of a 1.52 mm layer of Rogers RO4003. The patches are etched onto a 0.2 mm layer of FR4. These two layers are separated by a 5 mm layer of Avalon foam.

The FR4 is used for the accurate spacing of the patches in the array. The layer is as thin as possible as FR4 has high loss at 5.8 GHz. The foam spacer is used to obtain an even height for all the patches. The Rogers RO4003 is used for the feed as it has low loss [17]. The dimensions of the patch are shown in figure 4.2 and the layers in figure 4.3.

A linear polarized patch with a S_{11} below -10 dB, bandwidth of 300 MHz, a centre frequency of 5.8 GHz and 15 dB of gain is required. Side lobe levels of 13 dB below bore sight gain is acceptable. A pin fed patch with an input impedance of 100Ω was designed.

The bandwidth of a patch increases with increasing substrate thickness, decreasing ϵ_r and increasing width. A patch with a bandwidth of 10% is considered to be wideband. The ϵ_r of Avalon foam is close to that of air, so this cannot be reduced. The width of the patches cannot be increased as it is limited by the array spacing. It is further limited by the fact that the patches need to be linearly polarized. This only leaves the height of the patch which

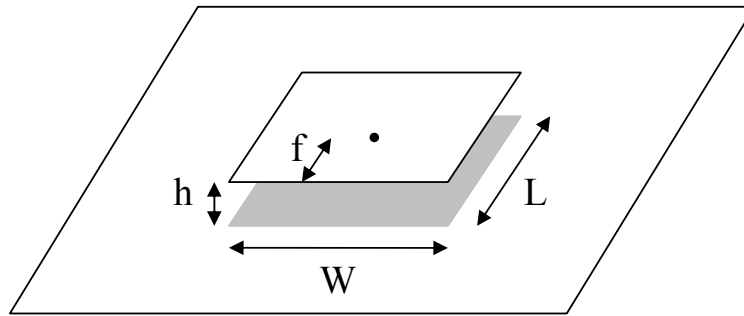


Figure 4.2: Definition of patch dimensions

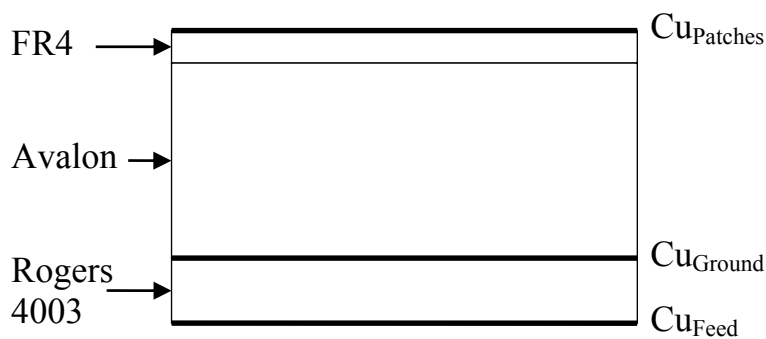


Figure 4.3: Layers used for the Patch

can be increased to increase the bandwidth. For a bandwidth of 10% the patch is 5 mm above the ground-plane. This causes a very high pin inductance, which needs to be compensated for.

The patches are designed as if they are on an air substrate. The foam used has similar properties to that of air, and the FR4 substrate is thin enough as not to affect the effective dielectric constant significantly [10].

On an air substrate, 10% patch-ground spacing, for a square patch, will result in a 20% bandwidth. For a narrow patch this bandwidth becomes approximately 10% [16]. The patches should, however, be narrow, at the expense of bandwidth, so that the patches can be spaced close together and for the higher input impedance. The patches should not be close to square as this leads to undesired polarisation problems.

If the patch is close to square, the patch can become resonant across its

width. This skews the polarisation of the patch, which can even become circular [18]. The width to length ratio of the patches is therefore chosen to be 80%.

A narrow patch that is high above the ground-plane should have the high input impedance and wide bandwidth specified. The high pin inductance is reduced by having the patch capacitive at the centre frequency and using thicker pins [16].

The design equations as given by Munson et al, equations 4.2 to 4.4, were used. Munson's equations are only accurate for a very thin substrate ($t \ll 0.01\lambda_f$) but can still be used as a starting point for thicker substrates.

$$\lambda_0 = \frac{c}{f} \quad (4.1)$$

$$L \approx 0.49\lambda_d \approx 0.49 \frac{\lambda_0}{\sqrt{\epsilon_r}} \quad (4.2)$$

$$R_m \approx \frac{60\lambda_0}{W} \quad (4.3)$$

$$R_{in} \approx R_m \cos^2 \frac{\pi x_0}{L} \quad (4.4)$$

Munson's equations give the parameters as $L = 25$ mm, $W = 20$ mm and $f = 5$ mm for $R_{in} = 100 \Omega$.

Due to the height of the patch above the ground-plane, the fringing fields are exaggerated, thus increasing the effective length of the patch. The patch therefore needs to be shortened and narrowed. The amount by which the patch is shortened is determined by simulating the patch as designed and then scaling the patch to move the centre frequency to 5.8 GHz.

The simulation shows a centre frequency of 4.8 GHz. The length of the patch is then multiplied by $\frac{4.8}{5.8}$, becoming 20.7 mm. The width is reduced to 16 mm. When this patch is re-simulated, the centre frequency is found to have moved to 5.75 GHz. It is well matched with a bandwidth of 9%. This patch is then used as the patch that is placed in the array, shown in Figure 4.4.

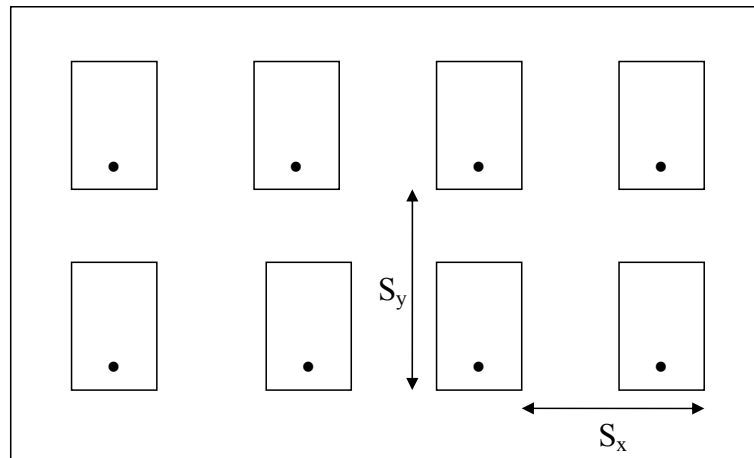


Figure 4.4: Antenna Spacing in the Array

4.1.1 Array

The single patch has a simulated gain of 8.8 dBi. A corporate feed is to be used to feed the antenna. This means that there needs to be 2^n elements in the array, where n is an integer. Increasing n by 1, increases the gain of the array by 3dB. For the 15 dB of specified gain, n should be 3. This means that 8 patches placed in a 2x4 array will suffice, giving 17.8 dB of gain. The 2x4 array results in a beam-width which is wider in one 'cut' than in the other. Because of the scanning nature of the radar, the narrower beam will be useful as it will give better angular resolution on the direction to the target.

The fact that the array is 2x4 means that an amplitude taper can be added to the array in the direction of the 4 patches. This could be implemented in a number of ways. The width of the patches could be changed so that they have different input impedances. Another method would be to change the feed position on the individual patches, but this would change the phasing as well as the amplitude of the patches. By using different line impedances and quarter wavelength transformers, the feed network can be changed so that the power does not divide equally at the junctions. Adding the amplitude taper will increase the beam-width and decrease the gain slightly. This could be used to suppress the side lobes of the radiation pattern. This is not implemented, as the antenna meets the 13 dB side lobe specification without the amplitude

taper.

When the patches are placed in an array there is mutual coupling between them, which changes the input impedances, as well as the centre frequency. The centre frequency of the patches, when simulated in the array, is found to be 6.1 GHz. This is corrected by lengthening the patches to 22 mm. The new array is simulated. The resulting centre frequency and the input impedance are shown to be acceptable.

The final dimensions for the patch array are given in Table 4-I. In order to prevent the formation of grating lobes, the spacing of the elements in the array is chosen as 80% of a free space wavelength.

Table 4-I: Final dimensions of Patch Antenna

Dimension	Value [mm]
Length	22
Width	16
Height	5
Feed	5
X	40
Y	40

4.2 Feed network

The feed is laid out on a 1.52 mm layer of Rogers RO4003, which has an ϵ_r of 3.38 and a $\tan \delta$ of 0.0027 [17]. Since the 0.2mm FR4 and the Avalon are flexible, the Rogers RO4003 is the only layer that provides the antenna with rigidity.

A corporate feed with quarter wave length transformers (QT) was used, giving the array uniform excitation. The layout of the the corporate feed is shown in Figure 4.5. The impedance of the feed is kept at 100Ω keeping the lines narrow to reduce the radiation from the feed network. The feed radiation can also be reduced by using 0.8 mm Rogers RO4003 for the feed, as this also

reduces the width of the lines. The reason for not doing this is that the thinner substrate is more flexible, and would lead to the entire antenna being flexible.

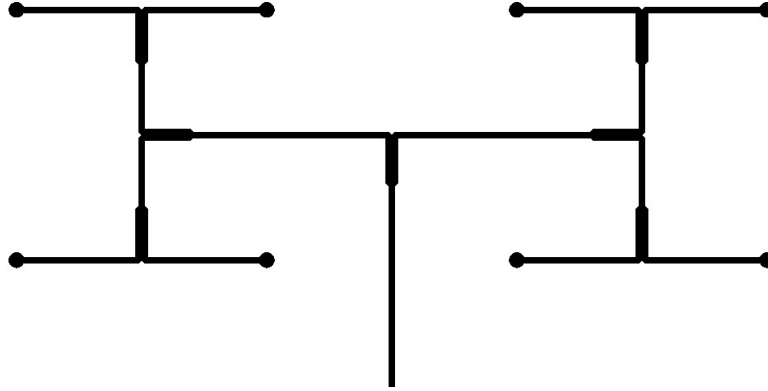


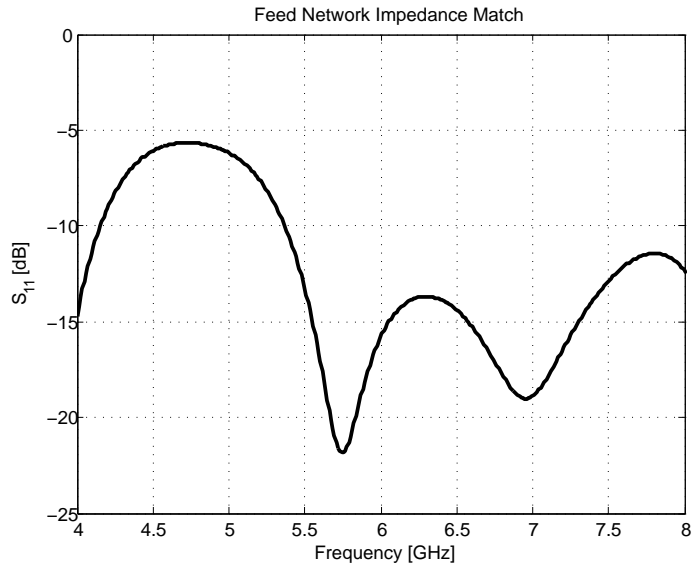
Figure 4.5: Feed Layout

Before the feed network is connected to the patches, it is simulated with 100Ω terminations where the patches are to be connected. This was also simulated for a 50Ω feed network. The 50Ω and 100Ω feed networks radiate 7, and 1.8% of the input power respectively. This confirms that the 100Ω feed network should be used. The input impedance of the 100Ω feed network was simulated. The results are shown in figure 4.6. They show that the bandwidth of the feed network is much more than that of the patch.

Equation 4.5 is used to calculate the characteristic impedance Z_t of a quarter wave length transformer used to match a line with impedance Z_0 to a load, or another line, with impedance Z_L . [10]

$$Z_t = \sqrt{Z_0 Z_L} \quad (4.5)$$

If the feed network impedance is 50Ω the impedance of two lines in parallel, (25Ω), would need to be transformed to 50Ω . This means a 35Ω transformer impedance. This gives a QT 8 mm long and 6 mm wide. If the feed impedance is 100Ω the QT needs to be 71Ω . This gives a QT with a length of 8 mm

Figure 4.6: S_{11} of feed network terminated with 100Ω loads

and a width of 1,9 mm. The reduction of the QT's width reduces the feed radiation, by reducing the fringing fields at the ends of the transformer.

Table 4-II gives the width for different Z_0 lines for a 1.52 mm Rogers RO4003 substrate

Table 4-II: Line width on 1.52mm Rogers RO4003

Z_0 [Ω]	width
35	6.0mm
50	3.5mm
71	1.9mm
100	0.9mm

The pins that are used to connect the patches to the feed network are wider than the 100Ω lines used to feed them, the transition from the microstrip line to the pin was therefore studied in more detail. The size of the hole and pad was swept from 2 mm to 3.5 mm and the results were compared, no guidelines

for these dimensions were found in literature. The dimensions for the pad and the ground hole diameters are chosen to be 2.4 mm and 4 mm, respectively.

4.3 Measurements

The antennas were measured in an anechoic chamber. The three antenna method was used to calculate the gain of the antennas. Three sets of measurements are made. Two of the antennas are placed a known distance apart and S_{21} is measured. The product of their gain is then calculated from the Friis equation, equation 4.6. This is repeated for all three combinations of the antennas, resulting in three equation for the three unknown gains. From these equations the gain of the individual antennas can be calculated [18].

$$\frac{P_r}{P_t} = G_{Tx}G_{Rx} \left(\frac{\lambda}{4\pi r} \right)^2 (1 - |\rho_{Tx}|^2) (1 - |\rho_{Rx}|^2) PLF \quad (4.6)$$

$$S_{21}S_{21}^* = \frac{P_r}{P_t} \quad (4.7)$$

The three antennas used are the transmit and receive patch antennas and one of the wide gain horns used in the proof of concept experiment, see sections 2.4 and 4.5. The measured results are plotted with the simulated results in figures 4.7, 4.8, and 4.9.

The measured gain is between 1 dB and 1.5 dB higher than the simulated gain, and the bandwidth is also slightly wider, at 1020 MHz and 960 MHz for the two measured antennas, and 820 MHz for the simulated antenna. At 5.8 GHz the antenna has measured gain of 18.6 dBi, compared to the simulated gain of 17.4 dBi. The increased bandwidth of the antennas might be as a result of the losses that are not included in the simulations. There are some differences between the S_{11} of the two antennas. This discrepancy is due to slight inaccuracies in the manufacturing process. One of the inaccuracies is that the patches are not flat due to the flexibility of the top layers (Avalon and FR4).

The radiation pattern is only measured in the cross polarized cut of the antenna. The results are plotted together with the simulated results in Figure 4.9. The slight angular offset between the measured and simulated results is

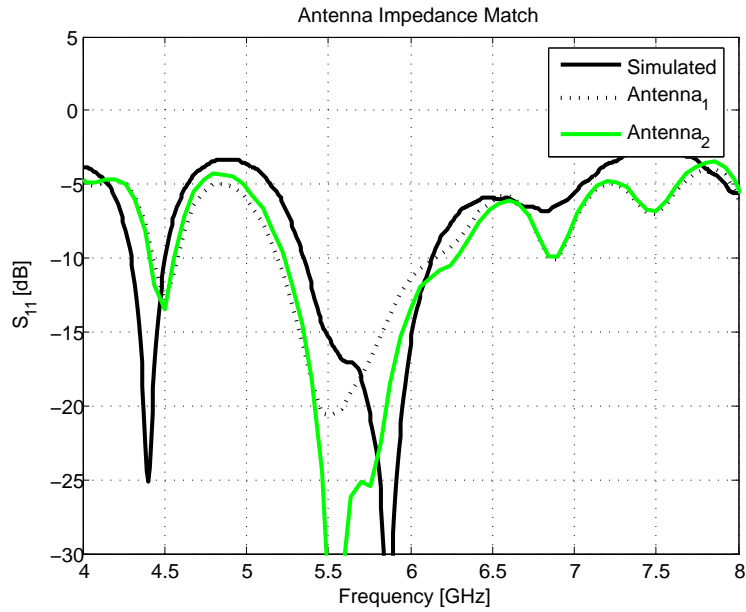
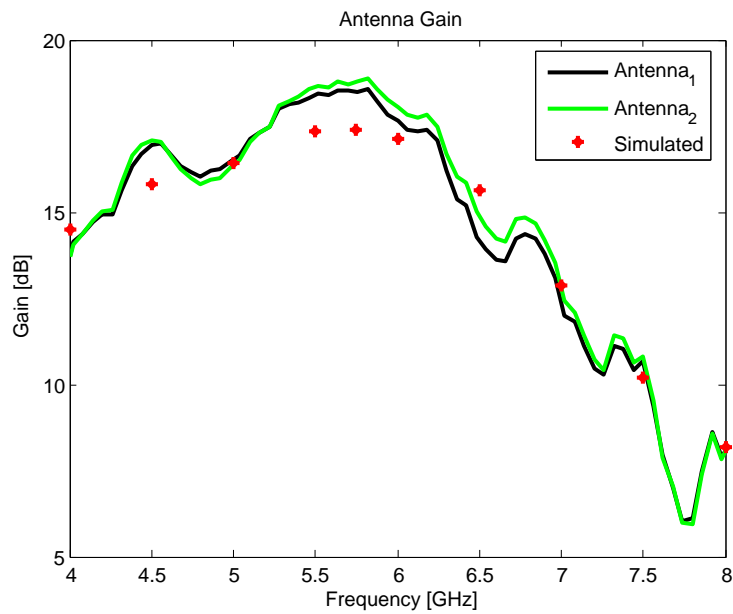
Figure 4.7: Measured and simulated S_{11} of patch array

Figure 4.8: Measured and simulated Gain of patch array

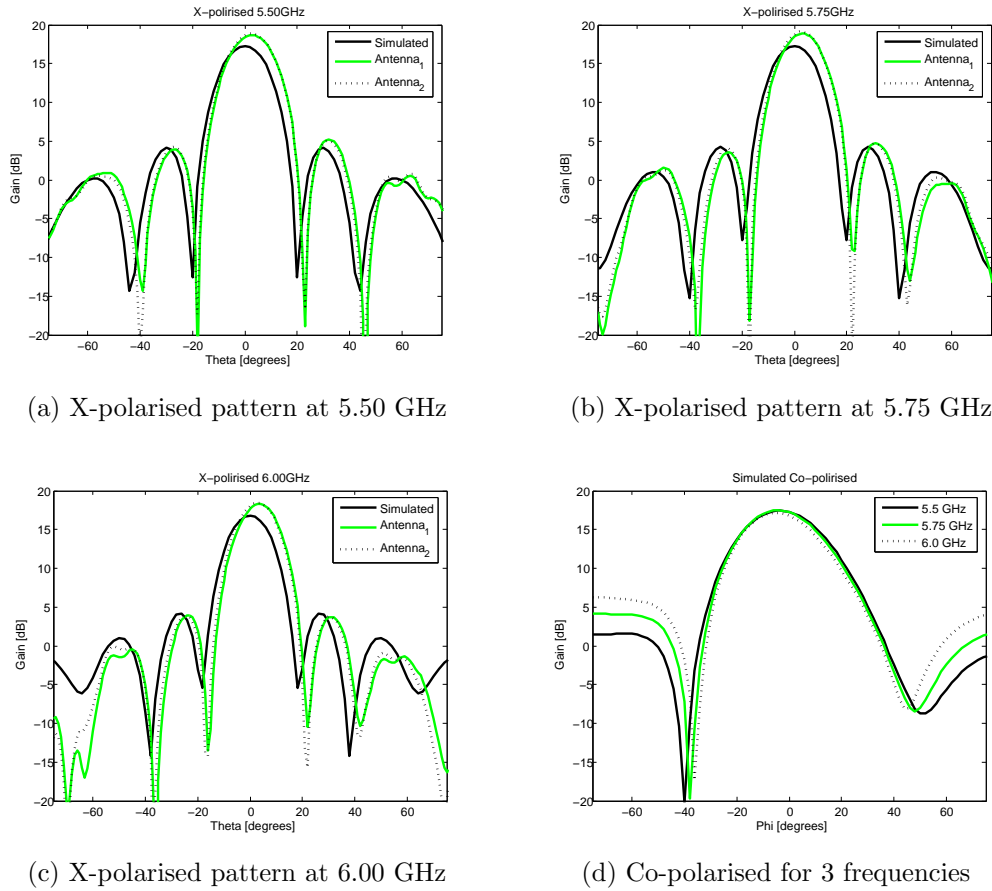


Figure 4.9: Measured Radiation Pattern of Patch Array

due to a slight miss-alignment of the antennas on the turn table. The radiation on the co-polarised cut was not measured, but the simulated results for the 3 frequencies are plotted in figure 4.9d.

4.4 Test Target

Three tri-hedral corner reflectors were made for the experiments so that the RCS of each target is known. The three reflectors have RCSs of 1.5 m^2 , 7.5 m^2 and 12 m^2 , respectively. The RCS of a Tri-hedral corner reflector can be calculated by Equation 4.8 [19].

$$RCS = \frac{12\pi r^4}{\lambda^2} \quad (4.8)$$

The RCS of a person is unknown, but is given by Skolnik [1] as being between 0.033 and 1.88 m^2 . In the final measurements of the system, the different targets, and a person, will be measured at a constant distance. The RCS of the person will be calculated from these results, see section 5.1.3 on page 62.

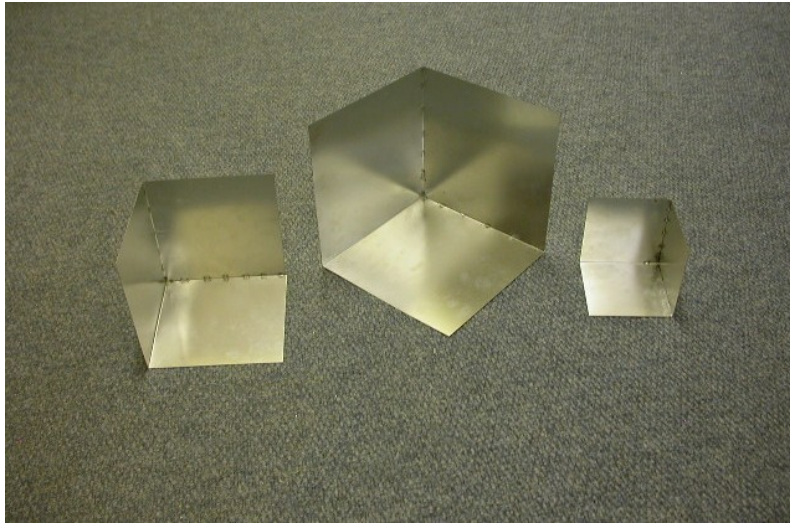


Figure 4.10: Photo of Tri-hedral corner reflectors

4.5 Other Antennas

Two wide band ridged horn antennas were used in the proof of concept measurements, see section 2.4. They have an operating frequency band from 2 to 18 GHz and have a gain of 12 dBi at 5.8 GHz.

Two cavity-backed bow-tie antennas with dielectric matching were used for the GPR [20]. The frequency range of these antennas is 50 to 400 MHz. The physical size of these antennas mean that they are quite far apart, approximately 1 m. As a result they require wide beams in order for the scattered power from a close in target to be received by the Rx antenna.

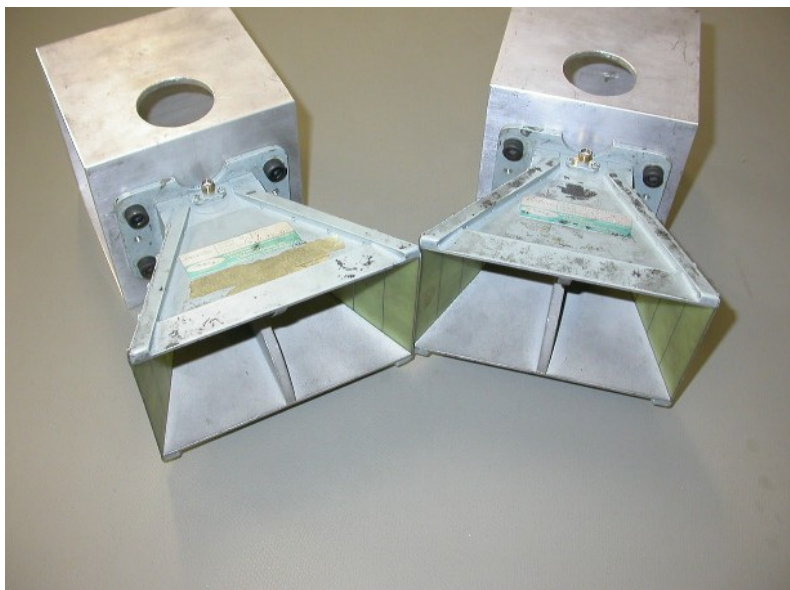
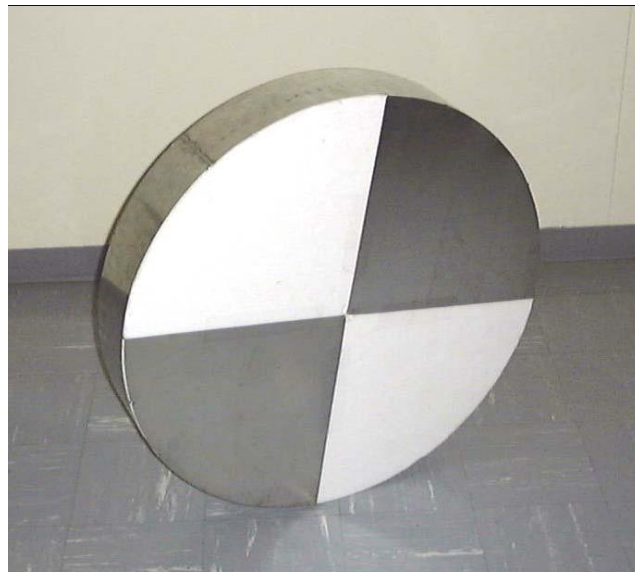


Figure 4.11: Photo of Horn Antennas



(a) Fully assembled Antenna



(b) Bottom view showing the bow-tie

Figure 4.12: Photos of GPR antenna

Chapter 5

Final Measurements

Two sets of measurements are presented. The first set of measurements were made using the pedestrian radar. The second set of measurements were made using the GPR.

For both sets of measurements the ADC was set up to sample at 2.5 MSPS and save 65 536 samples. This translates to 26.21 ms of continuous data, which is then split into 24 windows of 1.05 ms (T_{sweep}) each, of which 1 ms (T_{sample}) is used. The 24 windows are averaged. There is a visible transient in the sampled signal at each point where the frequency of the DDS is reset. These transients are used to determine where each of the windows starts.

5.1 Pedestrians

5.1.1 Setup

The system that is used for the first set of measurements is the system described by Figure 2.16 on page 27, reproduced here as figure 5.1.

The DDS is set up to sweep at a rate of 7.5 MHz/ms. The frequency is stepped 60 Hz every 8 ns, and is reset to 287.5 MHz every 1.05 ms. The DDS output frequency is then multiplied by 20 with the PLL. This gives a frequency sweep from 5.75 to 5.9 GHz, which means that the bandwidth of the system is 150 MHz. This satisfies the specification of 1 m resolution. The frequency to range conversion factor is 1 kHz/m. The transmit power of the system is 17 dBm and the receiver has 26 dB of gain. The SFC is included, at the output

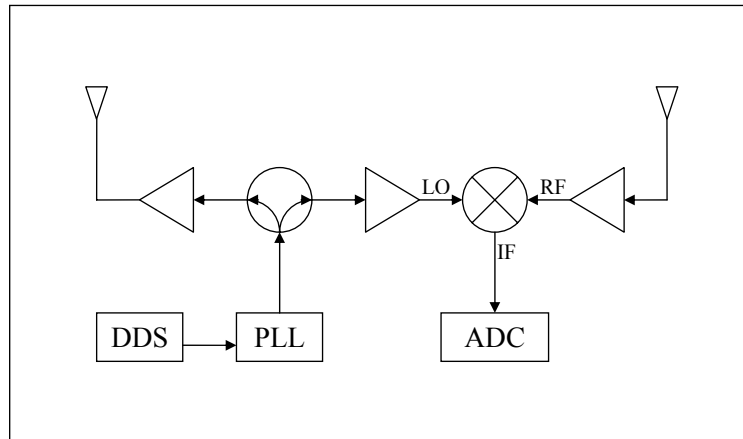


Figure 5.1: Block Diagram of radar

of the mixer.

The final measurements using the pedestrian radar was set-up on the section of roof next to the HF lab. The wall of the HF lab is approximately 3 m behind the radar.

There are two sets of measurements that were taken. In the first set of measurements the radar's antennas were rotated through 90° , with measurements taken at 5° intervals. The distance to the rails at the edge of the roof is measured. The area in front of the radar is shown in the photo in figure 5.2. A diagram of the roof is given in figure 5.3, the circle shows the position of a water tank, and the 'bang' shows the position of a solar panel and some other clutter. The position of the radar relative to the HF lab is shown in figure 5.4.

As the direction to which the radar is pointing changes the distance to the rails will increase. The increase in distance to the rails was measured.



Figure 5.2: Photo showing the area in front of the radar

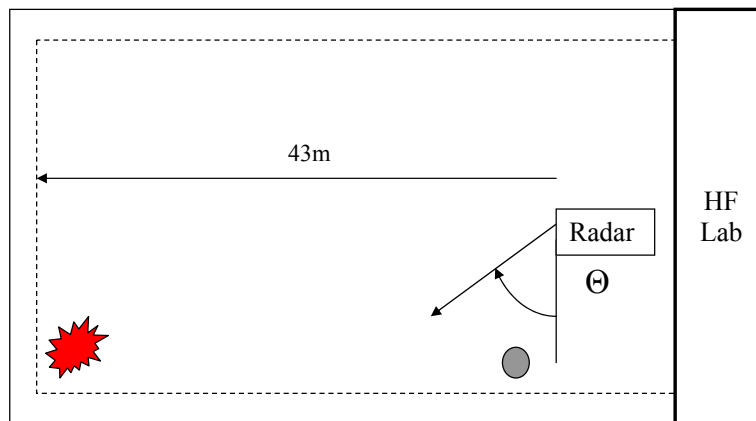


Figure 5.3: Diagram of the roof where the measurements were taken



Figure 5.4: Photo of the radar set-up showing the HF lab in the back ground

5.1.2 Results

Measurements were taken from $\theta = 45^\circ$ to $\theta = 135^\circ$ in 5° intervals. Two of the measurements, with $\theta = 60^\circ$ and 70° , are shown in figures 5.5 and 5.6 respectively. The distance to the rails at the radar's bore sight is expected to be 9 m and 16 m respectively.

In figure 5.5 there is a cluster of targets to be seen centred around 10 m with 2 m separation. The reason for seeing a cluster of targets, marked 'A', as opposed to a single target is that the individual posts supporting the rail is seen as different targets. The signal reflected off the rail itself is reflected away from the radar.

In figure 5.6 the cluster of targets have shifted from 10 m to 16 m and are approximately 10 dB smaller. The distance to the targets increases to the expected value of 16 m. The increase distance to the target from 10 m to 16 m should give a reduction in amplitude of 8.2 dB, which is close to the 10dB that has been measured.

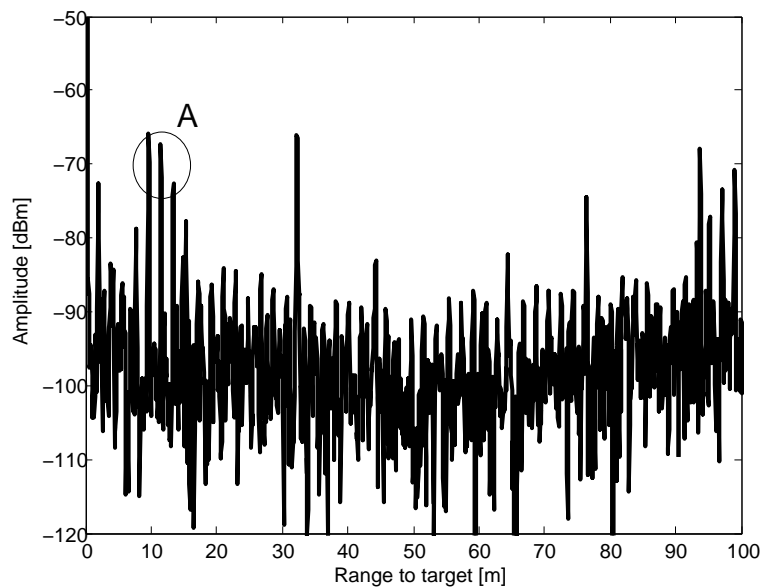
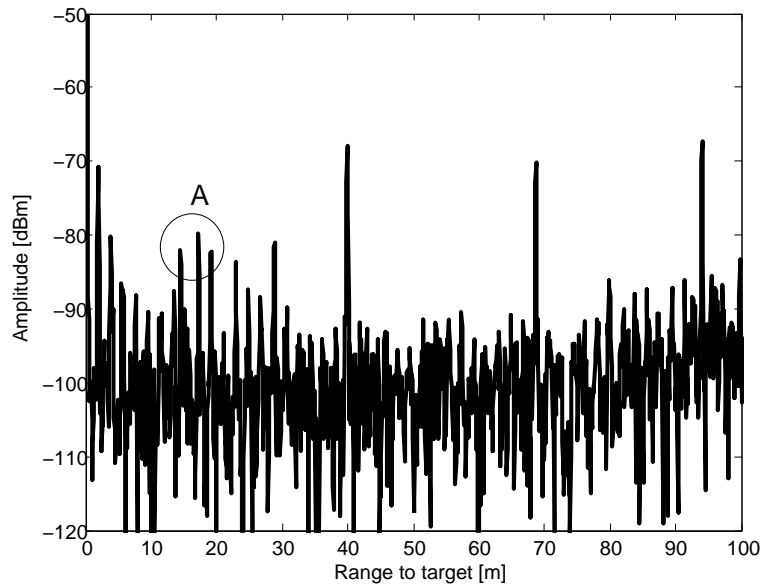


Figure 5.5: Measure Results with $\theta = 60^\circ$

Figure 5.6: Measure Results with $\theta = 70^\circ$

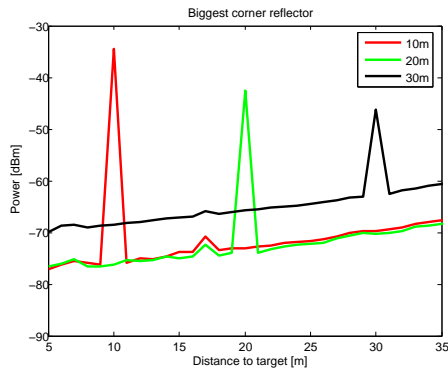
5.1.3 RCS Measurements

Measurements are taken at $\theta = 90^\circ$, with each of the targets discussed in section 4.4 placed at distances of 10 m, 20 m and 30 m. A fourth set of measurements are made with a person standing at the different distances. To remove the clutter of the rails a MTI is implemented. A measurement with no target on the roof is used as the reference. Figure 5.7 shows the measurement results. The distance to the targets is measured to the specified accuracy.

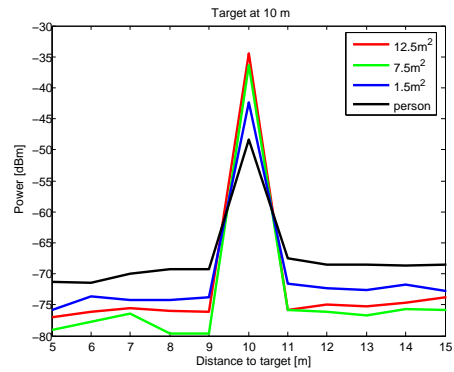
Figure 5.7a shows a rise in the noise floor with increasing frequency. This is caused by the SFC filter that suppresses the low frequency noise.

The measured and calculated Rx power for the different targets is presented in Table 5-I. The calculations are based on the radar equation (equation 2.15 on page 2.15), and the measured response of the SFC filter as presented in figure 3.8 on page 42. The data is processed using a square window.

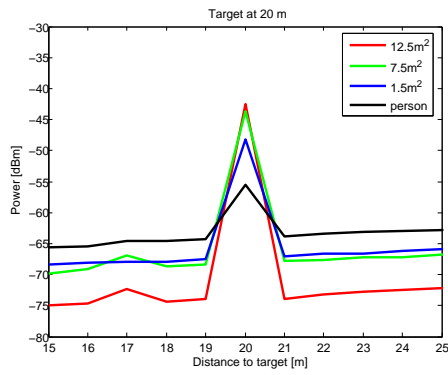
The measured amplitude of the reflections are 4 to 8 dB smaller than the calculated values. This is partially due to losses that are ignored. The targets may also appear smaller as a result of phase noise. The spectrum of the LO was measured and the results are presented in section 5.3.



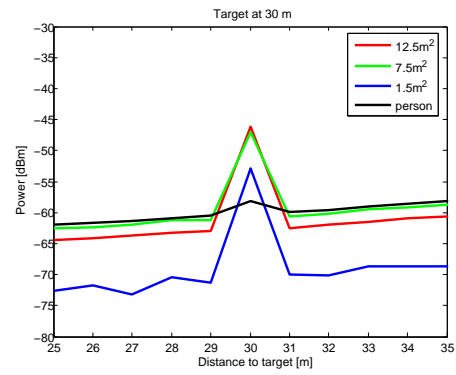
(a) Reflector at different distances



(b) Different targets at 10 m



(c) Different targets at 20 m



(d) Different targets at 30 m

Figure 5.7: RCS measurement results

Table 5-I: Expected and measured Rx power of the RCS Measurements in dBm

Target	10 m			20 m			30 m		
	Calc.	Meas.	Err.	Calc.	Meas.	Err.	Calc.	Meas.	Err.
12.5	-28	-33	5	-35	-43	8	-39	-46	7
7.5	-30	-36	6	-37	-44	7	-41	-47	6
1.5	-37	-43	6	-44	-48	4	-48	-54	6
Person		-48			-56			-58	

The reflection off the different reflectors are in proportion to their RCS. It can therefore be assumed that the RCS of the person is also in proportion to the reflected power, which is 4 to 8 dB smaller than that off the 1.5 m² target. This is used to calculate the RCS of the person to be between 0.23 m² and 0.6 m².

5.2 Ground Penetrating Radar

5.2.1 Setup

This system is identical to the system that was simulated, and presented in section 2.3. The block diagram for the GPR is shown in figure 2.1 on page 5, and is reproduced here in figure 5.8.

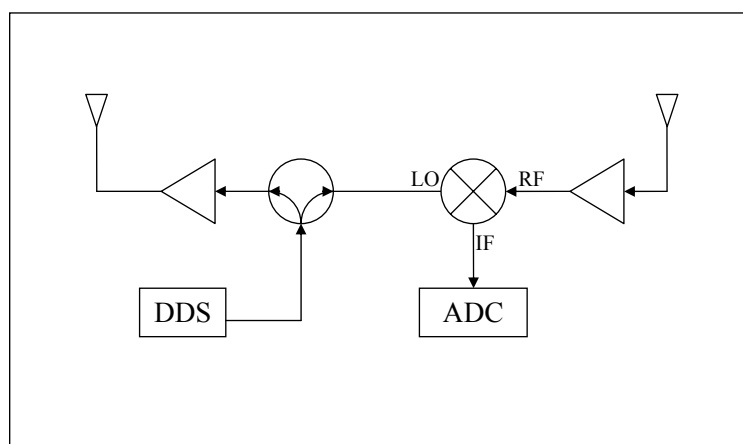


Figure 5.8: Block Diagram of simulated radar

The DDS is set to sweep from 50 MHz to 350 MHz in 1 ms. The transmit power is 9 dBm and the receiver has a gain of 22 dB.

The bandwidth of the system is 300 MHz, which gives a conversion of 2 kHz/m in air. In the ground the velocity of propagation is much slower, 10 cm/ns as opposed to 30 cm/ns in air [21]. The slower propagation causes increased time delay to the target and so the conversion factor becomes 6kHz/m.

The measurements are taken in the car park close to a manhole cover, the setuo is shown in figure 5.9. This was done in order to have a known target. A series of measurements were made, starting 5 m to the one side of the manhole cover and ending 3.4 m on the other. After each measurement is made the radar is moved 20 cm forward, giving a total of 44 measurements.



Figure 5.9: Photo of GPR measurement set-up.

Figures 5.10, 5.11 and 5.12 show the positions of the manhole cover and of the pipe, relative to the radar, for a selection of measurements.

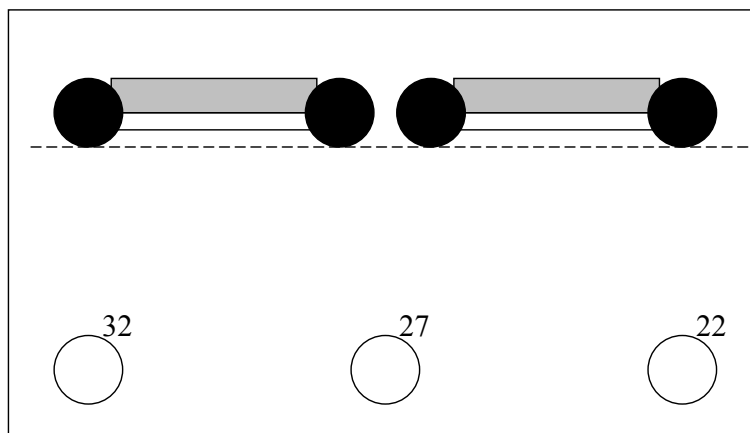


Figure 5.10: Position of antennas relative to storm water pipe.

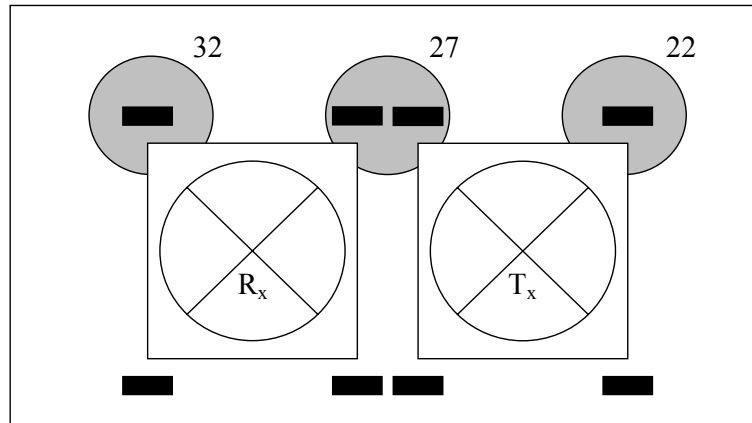


Figure 5.11: Position of antennas relative to manhole cover.

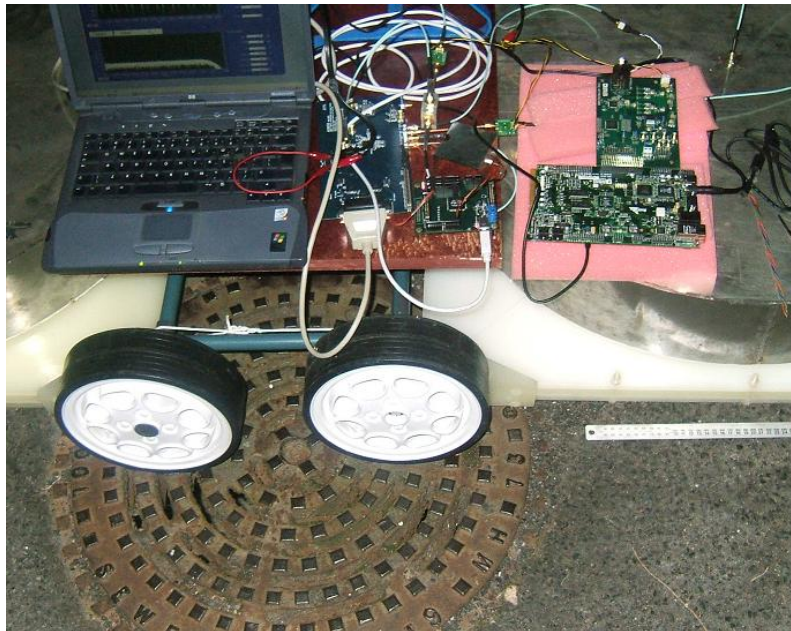


Figure 5.12: Photo of GPR system and the manhole cover in position 27.

5.2.2 Results

The 44 measured results are plotted vertically next to each other in figure 5.13. If there is a layered structure in the ground, the reflections will be at the same frequency in all of the measurements, which will be seen as horizontal lines in the plot. Point targets, like the pipe under the manhole cover, moves closer to the radar until the radar is directly above the target, then it moves away. This is seen as hyperbolic lines in the plot. These plots are clearer if the measurements are made at smaller spacings.

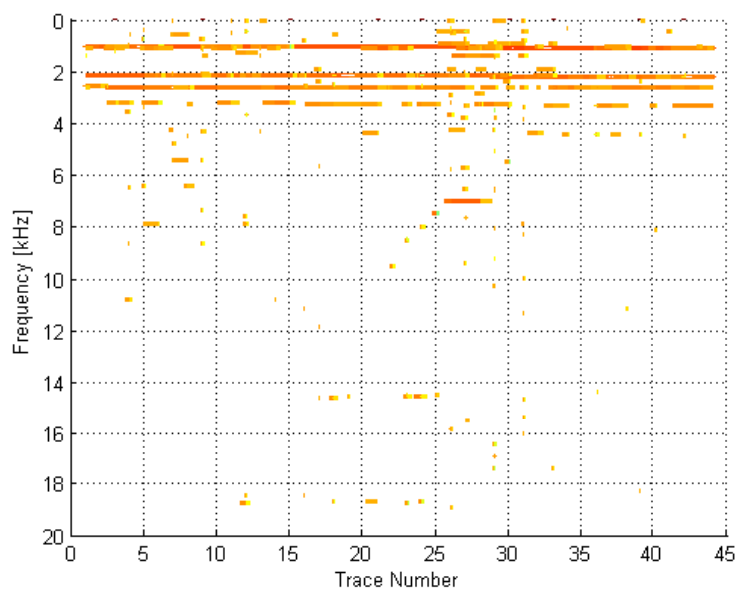


Figure 5.13: Measured results of GPR

There are 4 layers close to the surface that can clearly be seen, though one of these might be the coupling between the antennas. From trace 22 to 26 there is a target that moves from 9 to 7 kHz. This target then remains at 7 kHz for traces 26 to 29. A target at a frequency at 7 kHz is approximately 1.2 m under the surface. It can therefore be concluded that this target is the storm water pipe. The target is expected to go further, once the radar has passed over it, but it disappears. The reason for this is unknown.

The depth to the storm water pipe is 0.9 m, but it is measured as 1.2 m. The reason for this is that when we calculate the depth we assume that the Tx and Rx antennas are close together, and the velocity of propagation is approximated. What is actually calculated is that the signal propagates 2,4 m in the ground. In reality the centres of the antennas are 1.1 m apart. This means that the distance, from the one antenna to the pipe and back to the other antenna, is 2.4 m. This is two sides of a triangle, the third side is the distance between the antennas that is known to be 1.1 m. The height of the triangle (the depth of the target) can be recalculated to be 1 m, as shown in figure 5.14.

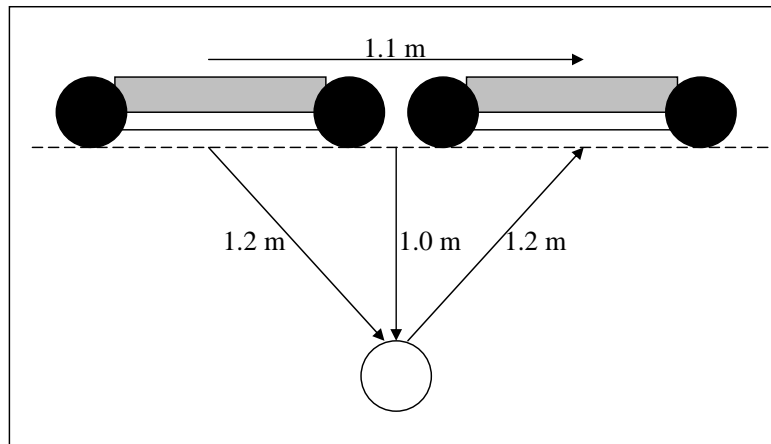


Figure 5.14: Target at 7 kHz corresponds to target at 1 m below the surface

There is a 246 kHz signal in all of the measurements. This corresponds to a target at 123 m in air, or approximately 41 m in the ground. Figure 5.15 shows the 246 kHz signal in two of the measurements. The source of this signal is unknown. The car park is in an area surrounded by buildings. This area is 40 m long, which could explain the presence of this target.

The targets are only 5 to 15 dB above the noise floor in the system. This is due to insufficient LNA gain and low Tx power.

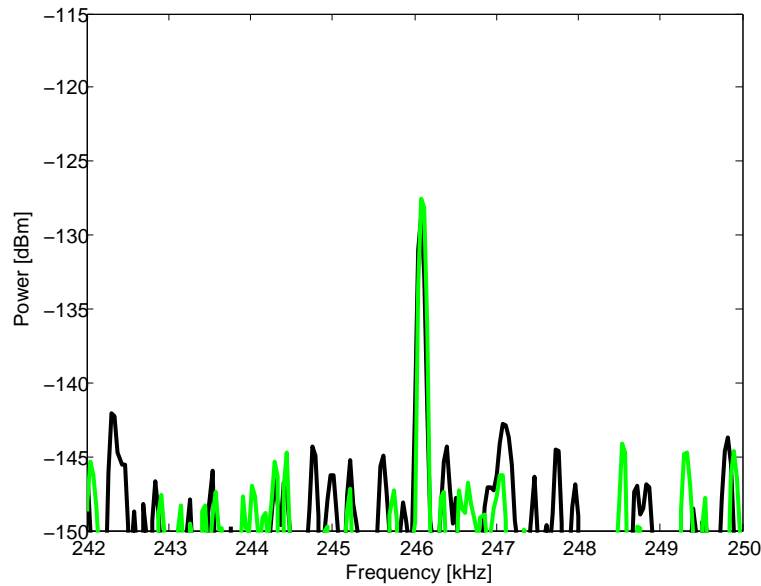


Figure 5.15: Target at 123 m in air or 41 m in ground

5.3 Local Oscillator

The RCS measurements were not as good as expected, see section 5.1.3 on page 62. The cause of the poor results is believed to be the phase noise of the LO. The spectrum of the LO was plotted in figure 3.4. In this measurement the LO was measured on its own, the power supply was therefore supplying much less current, as the rest of the system was not connected. The LO spectrum was re-measured while in the system and the spectrum is spread much wider than before. The measured results as well as the original measurements, of figure 3.4, are presented in Figure 5.16.

The cause of this increased phase noise, as well as spreading of the spectrum, is due to the noise on the power-supply of the LO. The noise on the power supply was less when the LO was measured on its own as less current was drawn from the power supply. To reduce the noise of the LO, a separate linear regulator is used to supply 3.3 V, regulated from the system 5 V supply. The spectrum was re-measured and is also plotted in figure 5.16.

The addition of the new voltage regulator improves the LO phase noise significantly, but it is still not as good as the original measurements when the

LO was measured on its own.

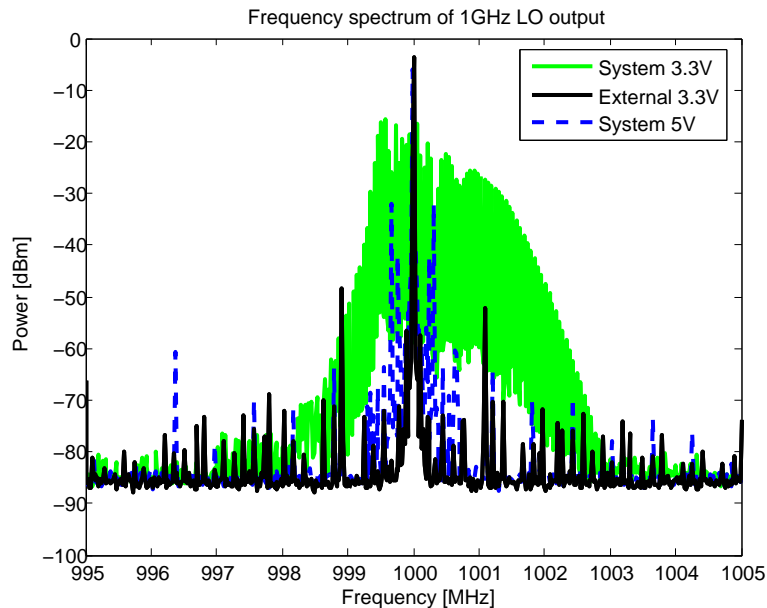


Figure 5.16: Measured spectrum of 1 GHz LO

5.4 Conclusion

Measurements were taken with each of the two systems and both are shown to work, although improvement is desirable.

The pedestrian radar's results compare well to the calculations, but the noise floor is higher than anticipated. The phase noise on the LO is found to be a possible cause for the increase noise in the system. This was improved by adding linear voltage regulators, but the improvement does not restore the phase noise to the levels measured when the LO was measured on its own. Different LOs should be investigated to determine whether this problem can be eliminated.

The results for the GPR are acceptable. It does not have the problems with phase noise as seen in the pedestrian radar. The GPR uses a bench power-supply, which provides quiet power with less noise than that of the pedestrian

radar. The signals that are received from the target at 1 m are only 10 dB above the noise floor of the system. This could be solved by using higher Tx power, more LNA amplification or averaging.

The systems' performance could be improved if they were to be laid out on custom PCBs. This will reduce ground loops and the resulting EMI issues.

Chapter 6

Conclusion

6.1 Conclusion

The design, simulation, and testing of two low cost FM-CW radars were discussed. These radars were built using off-the-shelf components which kept costs low without compromising performance.

The costs of the two radar systems are shown in tables 6-I and 6-II. There are two costs that are given, one for the system as it is built from the development/evaluation boards, and the other if the components were to be bought separately and mounted on a PCB.

Table 6-I: GPR Component Costs

Component	#	per Unit Cost		Total Cost		
		#	Development	Own PCB	Development	Own PCB
DDS	1		2825	450	2825	450
ADC	1		1225	350	1225	350
Amplifier	2		300	13	600	26
Splitter	1		549		549	0
FPGA	1		450	450	450	450
Antenna	2			100	200	200
Other	-			0	0	1000
Total	8				5849	1976

Other costs include PCB, voltage regulators, servo motor, etc. The cost for the antennas is an estimate for the C-band and the repair cost for the GPR antennas, which needed to have the transformers replaced.

Table 6-II: Pedestrian Radar Component Costs

Component	#	per Unit Cost		Total Cost	
		# Development	Own PCB	Development	Own PCB
DDS	1	2825	450	2825	450
ADC	1	1225	350	1225	350
PLL	1	1425	350	1425	350
Amplifier	4	630	23	2520	92
Splitter	1	367	35	367	35
FPGA	1	450	450	450	450
Antenna	2		100	200	200
Other	-		0	0	500
Total	8			9012	2427

It has been shown that the low cost components that were chosen can make a useful radar. Some care must be taken with the design and implementation of the system. Not all the specification were met, but the concept of using a DDS to implement a low cost FM-CW radar has been demonstrated. The maximum range of the system was not measured, but is in the range of 40 m for a person to be detected. The maximum range can be increased by adding more LNA gain to the receiver and ADC, the large signal that are received due to the antenna coupling will saturate some of the components if the gain is increased too much.

The use of evaluation boards is not recommended, as they are expensive. They also do not allow the user complete control of the components and the connections between the boards can lead to EMC/EMI problems. It is therefore recommended that the system should be laid out on a single PCB and all the components should be controlled form a central controller. Either a micro controller or an FPGA can be used. This not only gives the user complete control over the system, it also reduces the cost.

6.2 Further Development

As mentioned above, a PCB layout of the system will improve the system performance, by moving direct control of all the components to a central controller, as well as reducing EMI problems. The current system, excluding the antennas, shown in Figure 6.1 can be reduced to a single PCB, the size of the DDS development board.

The GPR could be laid out on a PCB in such a way that it can be deployed as a bore-hole radar. The GPR only draws 10 VA from the power-supply and so running it off a battery is viable.

The implementation of the SFC requires revision. As the frequency is below 1 MHz, an active filter should be considered as it will have a response that is closer to that of an ideal filter.

The simulations can be re-written in C⁺⁺ as this would make them much faster and more versatile. The simulation can then be used to investigate the effects of more parameters.

If an FPGA is to be used for the controller, it could also be used to process some of the data. This will mean that the system can be made independent of external control, which will make it suitable for development as a bore-hole radar. For the pedestrian radar the control of the servo motor can be included on the FPGA. The position of the platform can then be stored for each measurement.

The antenna can be improved by adding a tapered feed to reduce the side lobes. Higher gain will also give better accuracy to the directional measurements and will reduce clutter and multipath effects.

More advanced data processing techniques should be implemented for more information to be extracted from the data that is collected by the radar. The sweep rate of the signal can be made to vary. If this is done, and the data is processed correctly, much more data could be extracted from the system. One example is the speed of the target using the doppler frequency, which was ignored for the purposes of this project.

Since the components for this project were chosen and ordered, Analog Devices have released a new DDS that has more features than the AD9858. The use of this new DDS, the AD9910, would make the system more flexible and could increase the system performance.

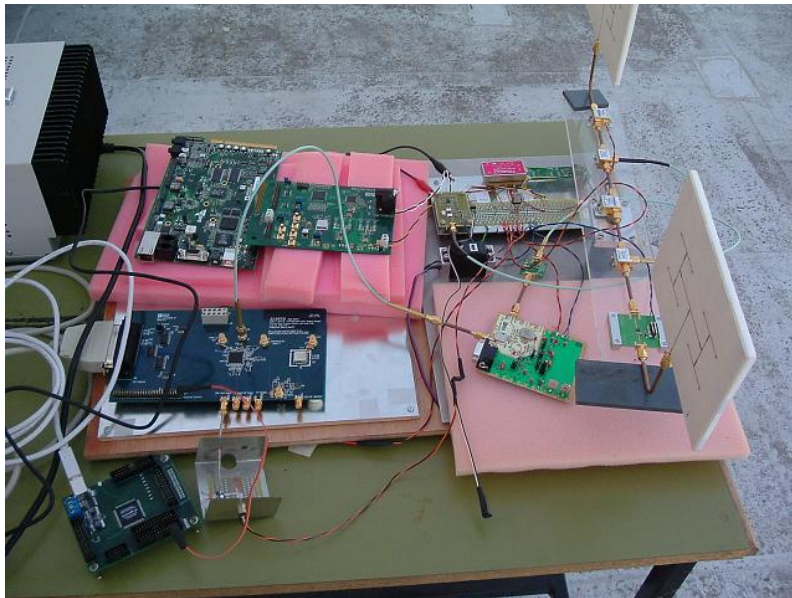


Figure 6.1: Pedestrian Radar System

Bibliography

- [1] Skolnik, M.I.: *Introduction to RADAR systems*. 3rd edn. Mc Graw-hill, 2001.
- [2] Daniels, D.J.: *Ground Penetrating RADAR*. 2nd edn. IEE, 2004.
- [3] Scheiblhofer, S. Schuster, S. Stelzer, A.: High-Speed FMCW Radar Frequency Synthesizer With DDS Based Linearization. *IEEE Microwave and Wireless Components Letters*, 2007.
- [4] Stove, A.: Linear FMCW Radar Techniques. *IEE Proceedings*, 1992.
- [5] Ellerbruch, D.A. Belsher, D.R.: Electromagnetic Technique of Measuring Coal Layer Thickness. *IEEE Transactions on Geoscience Electronics*, 1978.
- [6] Republic of South Africa: Licence free radio devices. Government Gazette, March 2004.
- [7] Musa, M. Salous, S.: Ambiguity Elimination in HF FMCW Radar Systems. *IEE Proceedings online*, 2000.
- [8] Skolnik, M.I.: *RADAR Handbook*. 2nd edn. Mc Graw-hill, 1990.
- [9] Proakis, J.G.: *Digital Signal Processing principles, algorithms, and applications*. 3rd edn. Wiley, 1996.
- [10] Pozar, D.M.: *Microwave engineering*. 3rd edn. Wiley, 2005.
- [11] Maas, S.: *Nonlinear Microwave and RF Circuits*. Artech House, 1997.
- [12] Moes, H.: *A Low Phase Noise PLL-Based Frequency Synthesiser For X-Band Radar - Draft*. Master's thesis, University of Stellenbosch, 2008.
- [13] Estmer, K.: *Noise Model of an FMCW Radar System*. Master's thesis, Jarfalla Royal Institute of Technology, 2002.

-
- [14] Laloue, A. Nallatamby, J. Prigent, M. Camiade, M. Obergon, J.: An Efficient Method for Nonlinear Distortion Calculation of the AM and PM Noise Spectra of FMCW Radar Transmitters. *IEEE transactions on Microwave Theory and Techniques*, 2003.
 - [15] Analog Devices: Sigma-Delta ADCs and DACs Application Note.
 - [16] Pozar, D.M.: A Review of Bandwidth Enhancement Techniques for Microstrip Antennas. *Microstrip Antennas*, pp. 157–166, 1995.
 - [17] Rogers Corporation: RO4003 Series High Frequency Circuit Material. 2006.
 - [18] Balanis, C.A.: *Antenna Theory analysis and design*. 3rd edn. Wiley, 2005.
 - [19] Fuhs, A.: *Radar Cross Section Lectures*. American Institute of Aeronautics and Astronautics, 1982.
 - [20] Birch, M.L.: *Development of a Cavity Backed Bowtie Antenna with Dielectric Matching for Ground Penetrating Radar*. Master's thesis, University of Stellenbosch, 2001.
 - [21] Annan, A.: *Ground Penetrating Radar workshop notes*, 2001.

Appendix A

Simulation Functions

The comment at the top of the function is used as a help file. The code in section A.1 is the radar system. It calls all the functions and sets all the inputs and then plots the results. The code, as presented, will produce the plot of the DDS v linear sweep as shown in figure 2.14 on page 24.

A.1 Radar Simulation

```

% J.G.Hoole
clc
clear all
close all

SimStart2 = clock;

% Radar system simulation.
LNAG = 10;
LNANF = -1;
AGCGmin = 10;
AGCGmax = 10;
AGCNF = -1;
Range = [10 20 30 40 50].*5.0;
RCS = [1 1 1 1 1].*1;
MaxRange = 1000;% [m]

MSPS = 2.5;
Tmin = 50000
Tsweep = 1050000;% [ns]

% DDS
% [L,time]=DDSapp(Pout,pstart,fmin,fmax,frate,ramp1,rampn,rampm,PhAmp)
[length1a,time1a]=DDSapp(0,0,100,257.5,8,Tsweep,1,1,0);
[length1d,time1d]=DDS(0,0,100,257.5,8,Tsweep,1,1,0);

% Radar Equation
% [delay,PRx]=RadarEqn(R,Gt,Gr,TxF,RCS,PTx);
[delay1a,PRx1a]=RadarEqn(Range(1),10,10,6,RCS(1),time1a);
[delay2a,PRx2a]=RadarEqn(Range(2),10,10,6,RCS(2),time1a);
[delay3a,PRx3a]=RadarEqn(Range(3),10,10,6,RCS(3),time1a);
[delay4a,PRx4a]=RadarEqn(Range(4),10,10,6,RCS(4),time1a);
[delay5a,PRx5a]=RadarEqn(Range(5),10,10,6,RCS(5),time1a);
[delay1d,PRx1d]=RadarEqn(Range(1),10,10,6,RCS(1),time1d);
[delay2d,PRx2d]=RadarEqn(Range(2),10,10,6,RCS(2),time1d);
[delay3d,PRx3d]=RadarEqn(Range(3),10,10,6,RCS(3),time1d);
[delay4d,PRx4d]=RadarEqn(Range(4),10,10,6,RCS(4),time1d);
[delay5d,PRx5d]=RadarEqn(Range(5),10,10,6,RCS(5),time1d);

% Add
PRxa = PRx1a + PRx2a + PRx3a + PRx4a + PRx5a;
PRxd = PRx1d + PRx2d + PRx3d + PRx4d + PRx5d;

% AGC
% [AGCout]=AGC(LNAG,LNANF,AGCGmin,AGCGmax,AGCNF,PRx)
[AGCouta]=AGC(LNAG,LNANF,AGCGmin,AGCGmax,AGCNF,PRxa);
[AGCoutd]=AGC(LNAG,LNANF,AGCGmin,AGCGmax,AGCNF,PRxd);

% Mix

```

APPENDIX A. SIMULATION FUNCTIONS

80

A.1. RADAR SIMULATION

```

Mixedda = time1a.*AGCouta/10;
Mixeddd = time1d.*AGCoutd/10;

% Filter
% [Fout]=ffilter(unF,freq)
[filtereda] = ffilter(Mixedda,10);
[filteredd] = ffilter(Mixeddd,10);

% Window
% [PRxw]=Window(MSPS,Tmin,Tsweep,Wtype,PRx)
[PRxwa]=Window(MSPS,Tmin,Tsweep,4,filtereda);
[PRxwd]=Window(MSPS,Tmin,Tsweep,4,filteredd);

%FFT and convert to dBm
FFTL = 2^20;
frdoa = fft(PRxwa,FFTL)/length1a/2;
frdo2a = frdoa.*conj(frdoa)/(2*50);
frdodBa = 10.*log10(frdo2a) + 30;
FFTL = 2^20;
frdod = fft(PRxwd,FFTL)/length1d/2;
frdo2d = frdod.*conj(frdod)/(2*50);
frdodBd = 10.*log10(frdod2d) + 30;

% save DDSplot.mat
% load DDSplot.mat

% Plot
fr = [MSPS:MSPS:FFTL*MSPS]/FFTL;

figure(6)
plot(1000*fr,frdodBa,'b','linewidth',2);hold on
plot(1000*fr,frdodBd,'r--','linewidth',2);
axis([0 350 -200 -130])
xlabel('Range to target [m]')
ylabel('Amplitude [dBm]')
title('Simulation Results of DDS v linear frequency sweep')
legend('Linear Sweep','DDS Sweep')

SimEnd = clock;

SimTime = SimEnd-SimStart2

```

A.2 DDS

```
function [L,time]=DDS(Pout,pstart,fmin,fmax,frate,ramp1,rampn,rampm,PhAmp);
```

```
% DDS simulation
%
% format: [length,time]=DDS(Pout,pstart,fstrt,fstop,...
% ...frate,ramp1,rampn,rampm,PhAmp);
%
% length      Length of signal      [ns]
% time        Time domain Output signal
%
% Pout        Output Power in 50 Ohm [dBm]
% pstart      Start Phase           [rad]
% fmin        Min Frequency          [MHz]
% fmax        Max Frequency          [MHz]
% frate       Frequency ramp time   [ns] minimum 8ns
% ramp1       Period of modulation  [ns]
% rampm       Type of modulation
%             -1 Saw tooth
%             0 Constant Frequency = fmax
%             1 Saw tooth
%             2 Triangle
%
% rampn       Number of periods of modulation
% PhAmp       Phase or amplitude output
%             0 Amplitude
%             1 Phase
```

```
% Code by J. G. Hoole
```

```
% December 2006
```

```
% Calculate amplitude from power
```

```
PoutWatt = 10^((Pout-30)/10);
```

```
A = sqrt(PoutWatt*2*50);
```

```
% convert 'frate' to a whole number
```

```
frate = floor(frate);
```

```
if frate < 8
```

```
    frate = 8;
```

```
end
```

```
% ensure that ramp1 is a multiple of frate
```

```
lerr = mod(ramp1,frate);
```

```
ramp1 = ramp1 - lerr;
```

```
% Calculate total length
```

```
length = ramp1*rampn + 1;
```

```
% calculate no. of frequency points
```

A.2. DDS

```

fnum = rampl/frate;

% calculate delta frequency
bandw = fmax - fmin;
dltaf = bandw/(fnum-1);

% convert frequency to phase per sample (ns)
% phps = 2*pi*freq/1000;

phase(1) = pstart;

if rampm == -1
    for k = 1:1:rampn
        for i = 1:1:fnum,
            freq = fmax - dltaf*(i-1);
            phps = 2*pi*freq/1000;
            for j = 1:1:frate,
                n = j + frate*(i-1) + rampl*(k-1);
                phase(n+1) = phase(n) + phps;
            end
        end
    end
elseif rampm == 0
    for i = 1:1:(lngth-1),
        freq = fmax;
        phps = 2*pi*freq/1000;
        phase(i+1) = phase(i) + phps;
    end
elseif rampm == 1
    for k = 1:1:rampn
        for i = 1:1:fnum,
            freq = fmin + dltaf*(i-1);
            phps = 2*pi*freq/1000;
            for j = 1:1:frate,
                n = j + frate*(i-1) + rampl*(k-1);
                phase(n+1) = phase(n) + phps;
            end
        end
    end
elseif rampm == 2
    freq = fmin;
    for k = 1:1:(rampn*2)
        d = (-1)^(k+1);
        for i = 1:1:fnum,
            phps = 2*pi*freq/1000;
            freq = freq + d*dltaf;
            for j = 1:1:frate,
                n = j + frate*(i-1) + rampl*(k-1);
                phase(n+1) = phase(n) + phps;
            end
        end
    end
end

```


A.2. DDS

```
        end
    end

    if PhAmp == 0,
        time = A.*cos(phase);
    else
        time = phase;
    end

    L = length(time);
```

A.3 Approximate DDS

```
function [L,time]=DDSapp(Pout,pstart,fmin,fmax,frate,ramp1,rampn,rampm,PhAmp);
```

```
% Approximate DDS simulation
%
% format: [length,time]=DDS(Pout,pstart,fstrt,fstop,...
% ...frate,ramp1,rampn,rampm,PhAmp);
%
% length    Length of signal        [ns]
% time      Time domain Output signal
%
% Pout      Output Power in 50 Ohm   [dBm]
% pstart    Start Phase              [rad]
% fmin      Min Frequency            [MHz]
% fmax      Max Frequency            [MHz]
% frate     Frequency ramp time     [ns] minimum 8ns
% ramp1     Period of modulation    [ns]
% rampn     Type of modulation
%           -1 Saw tooth
%           0 Constant Frequency = fmax
%           1 Saw tooth
%           2 Triangle
%
% rampn     Number of periods of modulation
% PhAmp     Phase or amplitude output
%           0 Amplitude
%           1 Phase
```

```
% Code by J. G. Hoole
```

```
% December 2006
```

```
% Pout = 30;%dBm
% pstart = 0;
% fmin = 200;
% fmax = 300;
% ramp1 = 10000;
% rampn = 5;
% rampm = 2;
```

```
% Calculate amplitude from power
```

```
PoutWatt = 10^((Pout-30)/10);
```

```
A = sqrt(PoutWatt*2*50);
```

```
fdta = abs(fmax - fmin);
```

```
t = 1:1:ramp1;
```

```
if rampm == -1
```

A.3. APPROXIMATE DDS

```

    phase = 2*pi*(fmax.*t - fdta/ramp1/2.*t.^2)/1000;
    ph = phase;
    for n = 1:1:(rampn-1)
        phase = unwrap([ph phase]);
    end
elseif rampm == 0
    w = 2*pi*fmax/1000
    phase = w.*(0:1:ramp1);
elseif rampm == 1
    phase = 2*pi*(fmin.*t + fdta/ramp1/2.*t.^2)/1000;
    ph = phase;
    for n = 1:1:(rampn-1)
        phase = unwrap([ph phase]);
    end
elseif rampm == 2
    ph1 = 2*pi*(fmax.*t - fdta/ramp1/2.*t.^2)/1000;
    ph2 = 2*pi*(fmin.*t + fdta/ramp1/2.*t.^2)/1000;
    if rampn ==1
        phase = ph1;
    else
        phase = [ph2 ph1]
    end
    ph = phase;
    for n = 1:1:(rampn-1)
        phase = unwrap([ph phase]);
    end
end

% ph3 = [0 phase];
% ph4 = [phase 0];
% fr = (ph4 - ph3)/2/pi*1000;
% plot(fr)
% axis([0 ramp1*rampn*2 fmin-100 fmax+100])

if PhAmp == 0,
    time = A.*cos(phase);
else
    time = phase;
end

L = length(time)

```

A.4 Radar Equation

```

function [delay,PRx]=RadarEqn(R,Gt,Gr,TxF,RCS,PTx);

% Loss due to radar range equation and propogation delay
%
% format:   [delay,PRx]=RadarEqn(R,Gt,Gr,TxF,RCS,PTx);
%
% delay     Propogation Delay
% PRx      Received signal
%
% R         Range to target

% Gt       Transmit Antenna Gain
% Gr       Receive Antenna Effective Area
% TxF      Transmit frequency [GHz]
% RCS      Radar cross section of Target
% PTx      Transmitted signal

% J.G. Hoole

c = 3e8;
lambda = c/(TxF*1e9);
Ae = Gr*lambda^2/(4*pi);

Gain = (Gt*RCS*Ae)/(16*(pi^2)*(R^4));% Power 'Gain' due to propogation
VGain = sqrt(Gain);% Voltage 'Gain' due to propogation

v = 3e8;
delay = round((2*R/v)*1e9);
L = length(PTx);

PRxd = [zeros(1,delay) PTx];

PRxt = PRxd(1,1:L);

PRx = PRxt.*VGain;

```

A.5 AGC

```

function [AGCout]=AGC(LNAG, LNANF, AGCGmin, AGCGmax, AGCNF, Rx);

% Automatic gain controll and LNA
%
% format:   [AGCout]=AGC(LNAG, LNANF, AGCGmin, AGCGmax, AGCNF, Rx);
%
% AGCout
%
% LNAG      LNA Gain           [dB]
% LNANF     LNA noise figure  [dB]
% AGCGmin   AGC minimum gain  [dB]
% AGCGmax   AGC maximum gain  [dB]
% AGCNF     AGC noise figure  [dB]
% Rx        Input signal

PRx = (mean((Rx.^2)))/50;

PRxdBm = 10*log10(PRx)+30;

AGCG = -30-PRxdBm;

if AGCG < AGCGmin
    AGCG = AGCGmin;
elseif AGCG > AGCGmax
    AGCG = AGCGmax;
else
    AGCG = AGCG;
end

Gain = LNAG + AGCG;% total Gain

VGainLNA = 10.^(LNAG/20);
VGainAGC = 10.^(AGCG/20);

Rx1 = Rx.*VGainLNA;

[LNAout]=Noise(LNAG, LNANF, Rx1);

Rx2 = LNAout.*VGainAGC;

[AGCout]=Noise(AGCG, AGCNF, Rx2);

```

A.6 Filter

```
function [Fout]=ffilter(unF,freq)

% RC low pass filter
% format:  [Fout]=ffilter(unF,freq)
%
% Fout      Filtered Output
%
% unF       unfiltered input
% freq      Cutoff frequency of filter [MHz]

tau = 1000/(2*pi*freq);

Tend = floor(5*tau)

% filter
t = 0:1:Tend;
a = 1/tau.*exp(-t/tau);
Fout = conv(a,unF);
```

A.7 Window and sampling

```

function [PRxw]=Window(MSPS,Tmin,Tsweep,Wtype,PRx);

% format: [PRxw]=Window(MSPS,Tmin,Tsweep,Wtype,PRx);
%
% PRxw      Sampled, windowed received signal
%
% MSPS      Sampling rate [MSPS]
% Tmin      Delay to furthest target
% Tsweep    Sweep time
% Wtype     Type of window
%           0 - Square
%           1 - Hanning
%           2 - Hamming
%           3 - Blackman
%           4 - 4-term Blackman Harris
%
% PRx      Receive signal

Tsample = floor(1000/MSPS);% ns per sample

if Tsample == 0
    Tsample = 1;
end

j = 1;
for i = Tmin:Tsample:Tsweep;
    PRxs(j) = PRx(i);
    j = j + 1;
end

M = length(PRxs);

if Wtype == 0

    PRxw = PRxs;

elseif Wtype == 1

    % Hanning window
    for n = 1:1:M
        a = 0.5 - 0.5*cos(2*pi*n/M);
        PRxw(n) = a*PRxs(n);
    end

elseif Wtype == 2

    % Hamming window
    for n = 1:1:M
        a = 0.54 - 0.46*cos(2*pi*n/M);

```

APPENDIX A. SIMULATION FUNCTIONS
A.7. WINDOW AND SAMPLING

90

```
        PRxw(n) = a*PRxs(n);
    end

elseif Wtype == 3

    % Blackman window
    for n = 1:1:M
        a = 0.42 - 0.5*cos(2*pi*n/M) + 0.08*cos(4*pi*n/M);
        PRxw(n) = a*PRxs(n);
    end

elseif Wtype == 4

    % 4-term Blackman Harris window
    a0 = 0.35875;
    a1 = 0.48829;
    a2 = 0.14128;
    a3 = 0.01168;
    for n = 1:1:M
        a = a0 - a1*cos(2*pi*n/M) + a2*cos(4*pi*n/M) - a3*cos(6*pi*n/M);
        PRxw(n) = a*PRxs(n);
    end

end
```